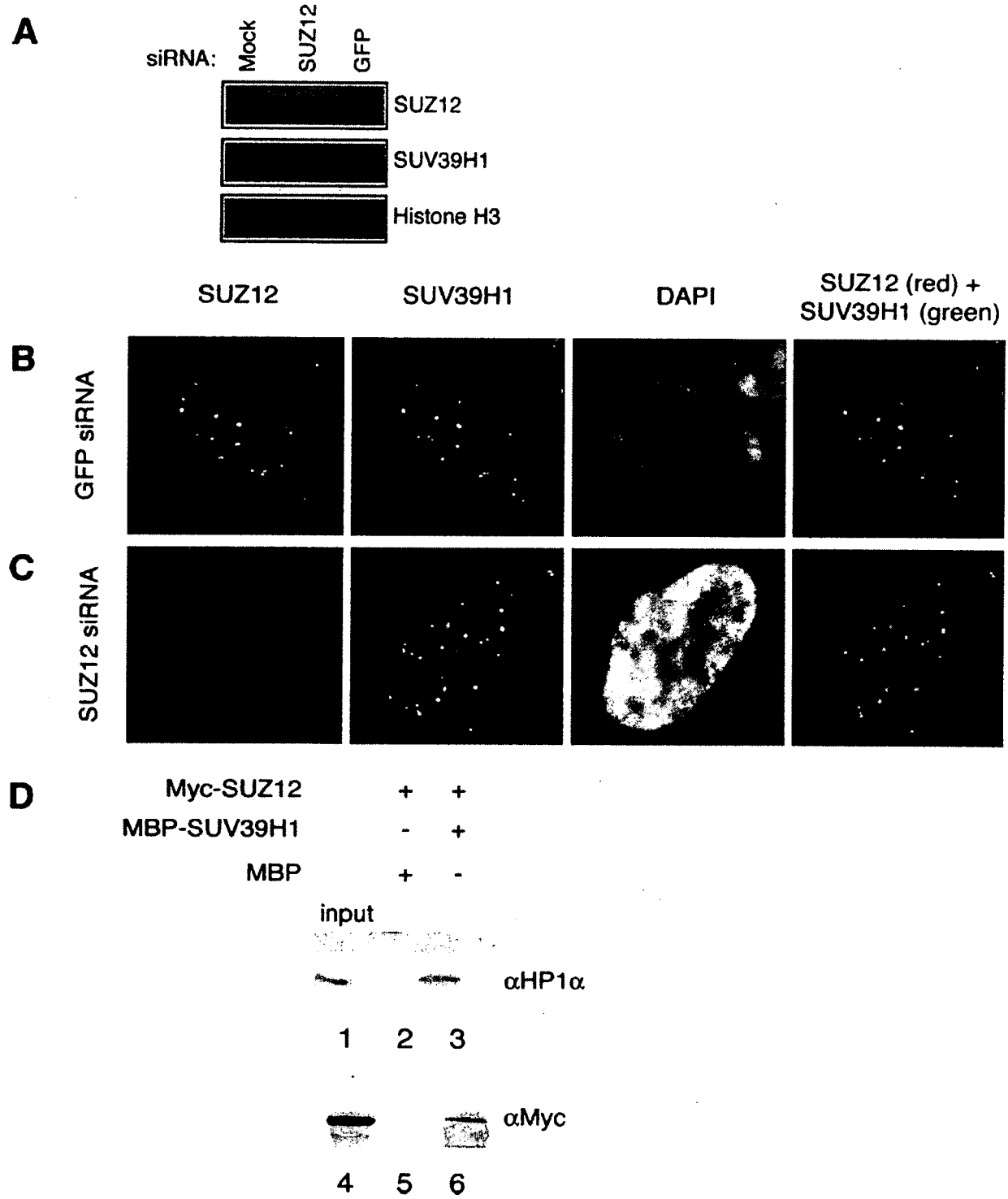

Figure 6. Distribution of SUZ12 and SUV39H1 in SUZ12 knockdown cells. **A**: Western blotting for SUZ12, SUV39H1, and gamma tubulin IMR90 cells transfected with no siRNA, SUZ12 siRNA, or GFP siRNA. **B,C**: Immunostaining for SUZ12 (first column) and SUV39H1 (second column) in IMR90 cells treated with GFP siRNAs (**B**) or SUZ12 siRNAs (**C**). Nuclei are stained with DAPI (third column) and the merged panel (fourth column) consists of SUZ12 (red) and SUV39H1 (green). **D**: Association of SUZ12 and SUV39H1. Cell extracts containing Myc-SUZ12 were incubated with either MBP-tagged SUV39H1 (lanes 3 and 6) or MBP alone (lanes 2 and 5). MBP-SUV39H1 (lane 3) but not MBP (lane 2), interacts with HP1α from cell lysates. Myc-SUZ12 was specifically pulled down by MBP-SUV39H1 (lane 6).

pared to the GFP siRNA treated cells (Figure 5A–C). In contrast, there was no noticeable increase in micronuclei formation in EZH2 knockdown cells (data not shown). These results suggest that centromere function is perturbed in SUZ12 knockdown cells.

SUV39H1 levels are not altered in SUZ12 knockdown cells

In mammalian somatic cells, SUV39H1 is the major HMTase that mediates tri-methylation of H3-K9. We performed Western blot analyses on mock transfected, GFP siRNA transfected, and SUZ12 siRNA transfected cells to determine if loss of this methyl mark in SUZ12 knockdown cells was due to a decrease in levels of SUV39H1. SUV39H1 was present in similar amounts in control and SUZ12 siRNA transfected cells, indicating that SUZ12 knockdown did not substantially alter the levels of SUV39H1 (Figure 6A). Next, immunostaining was used to assay whether the distribution of SUV39H1 was affected in SUZ12 siRNA-treated cells. In GFP siRNA-treated cells, SUV39H1 was found in many speckles of variable intensity scattered throughout the nucleus (Figure 6B). Distribution of SUV39H1 was not detectably altered in cells lacking SUZ12 (Figure 6B). Together these data indicate that the altered levels of H3K9me3 detected in SUZ12 knockdown cells were not due to a loss or aberrant localization of SUV39H1 (Figure 6C).

Analysis of SUZ12 and SUV39H1 distribution in IMR90 cells revealed that SUZ12 co-localized with SUV39H1 in a subset of large, bright speckles (Figure 6B), suggesting that these two proteins may associate. To test this hypothesis we performed pull-down experiments. Recombinant MBP-SUV39H1 was incubated with 293 HEK cell extracts over-expressing Myc-tagged SUZ12. *In vitro* binding assays using amylose-conjugated sepharose beads were performed. The precipitates were analyzed for the presence of HP1α and Myc-tagged SUZ12 by Western blotting. Recombinant MBP-SUV39H1 exhibited histone methyltransferase activity (data not shown) and HP1α binding activity (Figure 6D, compare lanes 2 and 3; (Aagaard *et al.* 1999, Grewal & Moazed 2003, Melcher *et al.* 2000, Yamamoto & Sonoda 2003), indicating that the protein was functional. Myc-SUZ12 was enriched in the MBP-SUV39H1 pull-down sample when compared to MBP alone (Figure 6D, compare lanes 5 and 6). Thus, SUV39H1 can precipitate SUZ12 in addition to HP1α.

Discussion

We have identified a role for the PcG protein SUZ12 in regulating levels of H3K9me3 in differentiated cell types. Differentiation of *Suz12* −/− ES cells resulted in a reduction of H3K9me3. Depletion of SUZ12 in human fibroblasts resulted in a loss of H3K9me3, without affecting the abundance or distribution of the H3K9me3 HMTase SUV39H1. HP1α was redistributed upon SUZ12 depletion, consistent with the role of H3K9me3 in the correct localization of HP1α (Lachner *et al.* 2001, Peters *et al.* 2001, 2003, Rice *et al.* 2003). Knockdown of SUZ12 led to an increase in the proportion of cells with micronuclei and chromatin bridges, likely due to a defect in chromosome segregation due to perturbation of H3K9me3/HP1α at constitutive heterochromatin (Peters *et al.* 2001). In contrast, knockdown of EZH2 did not change the amounts of H3K9me3, indicating that SUZ12 acts independently of EZH2 in regulation of H3-K9 tri-methylation. We conclude that SUZ12 has EZH2-dependent and EZH2-independent activities that regulate H3K27me3 and H3K9me3/HP1α-containing heterochromatin respectively. Thus, SUZ12/Suz12 is critical for correct formation of both constitutive heterochromatin and facultative heterochromatin in differentiated mammalian cells.

In a recent study knockdown of SUZ12 in HeLa cells had no discernible effect on H3K9me3 levels, when assayed by Western blot (Cao & Zhang 2004b), indicating that SUZ12 does not regulate H3-K9 tri-methylation in this transformed human cell type. In contrast, we observed a 2-fold decrease in bulk H3K9me3 levels upon SUZ12 knockdown in primary human cells. In addition, our single-cell analysis revealed that only cells completely lacking SUZ12 exhibited dramatic depletion of H3K9me3, an effect observed in three different human primary cell lines. The different effects of SUZ12 depletion on H3K9me3 levels in HeLa cells and primary human fibroblasts could be due to differences in cell type, knockdown procedures, or method of analysis. In fibroblasts, H3K9me3 levels were less sensitive than H3K27me3 to SUZ12 knockdown, as a

decrease in amounts of H3K27me3 could be detected after 3 days of siRNA treatment (data not shown), while the H3K9me3 phenotype was only apparent after 6 days after siRNA treatment. This lag may be due to differences in stability of H3K9me3 versus H3K27me3.

The interaction between HP1 proteins and the SUV39H family of HMTases plays a role in propagation of H3-K9 methylation (Grewal & Moazed 2003). Our results indicate that SUZ12 co-localizes with a subset of SUV39H1 foci, and that these proteins interact *in vitro*. SUZ12 also interacts with HP1α *in vitro* and SUZ12 and HP1α co-localize in HeLa cells (Yamamoto *et al.* 2004). This suggests that the decrease in H3K9me3 and the redistribution of HP1α observed upon SUZ12 knockdown may occur because SUZ12 directly regulates SUV39H1 and/or HP1α function. A second possibility is that SUZ12 regulates the HP1α/SUV39H1 interaction that is necessary for propagation of H3K9me3. Alternatively, SUZ12 may be necessary to inhibit the activity of the H3K9me3 demethylase, JMJD2B (Fodor *et al.* 2006).

The differentiation-dependence of the effect of the *Suz12* mutation on H3K9me3 but not H3K27me3 suggests that Suz12 may function primarily in the Eed/Ezh2 complexes in ES cells and in regulating the activity of H3K9me3 HMTase complexes in differentiated cells. Mammals have two H3K9me3 HMTases, SUV39H1 and SUV39H2. Perhaps the differentiation-dependence of Suz12 in regulation of H3K9me3 levels reflects a role for Suz12 in regulation of only one of these two HMTases, which exhibit different expression patterns in differentiated cell types (O'Carroll *et al.* 2000). Alternatively, Suz12 may regulate H3K9me3 demethylase activity exclusively in differentiated cells.

SUZ12 expression is mis-regulated in many human cancers, implicating SUZ12 in regulation of cell proliferation (Kirmizis *et al.* 2003). SUZ12 knockdown alters H3-K27 methylation and expression of SUZ12 target genes, such that changes in SUZ12 levels may perturb the expression of genes essential for normal growth and proliferation (Kirmizis *et al.* 2003). Our data also implicate SUZ12 in regulation of constitutive heterochromatin in primary cells, suggesting that defects in SUZ12-dependent chromatin may also contribute to tumorigenesis by increasing genomic instability. Indeed, a high proportion of SUZ12 knockdown cells exhibit micronuclei and chromatin bridges, which correlate with aneuploidy (Jallepalli & Lengauer 2001). Our study demonstrates that the dual functions of SUZ12 in regulating both facultative and constitutive heterochromatin may be essential for maintaining appropriate gene expression as well as genomic integrity.

Acknowledgements

We thank Hiten Madhani, Shiv Venkatasubrahmanyam, and our colleagues in the Panning Laboratory for their enlightening discussions and critical reading of the manuscript. We are grateful to Judith Sharp, Tom Fazzio, Dmitri Nusinow, Jason Huff, and Dale Talbot for their excellent technical advice and assistance. We acknowledge Brian Biehs for his limitless patience. The methyl histone antibodies were a gift from Yi Zhang. B.P. is a Pew Scholar and is funded by NIH and by grants from the Sandler Family Foundation. C.C.C. was a recipient of a National Sciences Foundation pre-doctoral fellowship and a University of California Office of the President, Dissertation Year Fellow.

References

Aagaard L, Laible G, Selenko P *et al.* (1999) Functional mammalian homologues of the Drosophila PEV-modifier Su(var)3-9 encode centromere-associated proteins which complex with the heterochromatin component M31. *Embo J* **18**: 1923–1938.

Bannister AJ, Zegerman P, Partridge JF *et al.* (2001) Selective recognition of methylated lysine 9 on histone H3 by the HP1 chromo domain. *Nature* **410**: 120-124.

Birve A, Sengupta AK, Beuchle D *et al.* (2001) Su(z)12, a novel Drosophila Polycomb group gene that is conserved in vertebrates and plants. *Development* **128**: 3371–3379.

Breiling A, O'Neill LP, D'Eliseo D, Turner BM, Orlando V (2004) Epigenome changes in active and inactive Polycomb-group-controlled regions. *EMBO Rep* **5**: 976–982.

Cao R, Zhang Y (2004a) The functions of E(Z)/EZH2-mediated methylation of lysine 27 in histone H3. *Curr Opin Genet Dev* **14**: 155–164.

Cao R, Zhang Y (2004b) SUZ12 is required for both the histone methyltransferase activity and the silencing function of the EED-EZH2 complex. *Mol Cell* **15**: 57–67.

Cao R, Wang L, Wang H *et al.* (2002) Role of histone H3 lysine 27 methylation in Polycomb-group silencing. *Science* **298**: 1039–1043.

Cheutin T, McNairn AJ, Jenuwein T, Gilbert DM, Singh PB, Misteli T (2003) Maintenance of stable heterochromatin domains by dynamic HP1 binding. *Science* **299**: 721–725.

Czermin B, Melfi R, McCabe D, Seitz V, Imhof A, Pirrotta V (2002) Drosophila enhancer of Zeste/ESC complexes have a histone H3 methyltransferase activity that marks chromosomal Polycomb sites. *Cell* **111**: 185–196.

de la Cruz CC, Fang J, Plath K *et al.* (2005) Developmental regulation of Suz 12 localization. *Chromosoma* **114**: 183–192.

Erhardt S, Su IH, Schneider R *et al.* (2003) Consequences of the depletion of zygotic and embryonic enhancer of zeste 2 during preimplantation mouse development. *Development* **130**: 4235–4248.

Festenstein R, Pagakis SN, Hiragami K, Lyon D, Verreault A, Sekkali B, Kioussis D (2003) Modulation of heterochromatin protein 1 dynamics in primary Mammalian cells. *Science* **299**: 719–721.

Fodor BD, Kubicek S, Yonezawa M *et al.* (2006) Jmjd2b antagonizes H3K9 trimethylation at pericentric heterochromatin in mammalian cells. *Genes Dev* **20**: 1557–1562.

Fujimura Y, Isono K, Vidal M *et al.* (2006) Distinct roles of Polycomb group gene products in transcriptionally repressed and active domains of Hoxb8. *Development* **133**: 2371–2381.

Grewal SI, Moazed D (2003) Heterochromatin and epigenetic control of gene expression. *Science* **301**: 798–802.

Hayakawa T, Haraguchi T, Masumoto H, Hiraoka Y (2003) Cell cycle behavior of human HP1 subtypes: distinct molecular domains of HP1 are required for their centromeric localization during interphase and metaphase. *J Cell Sci* **116**: 3327–3338.

Hoffelder DR, Luo L, Burke NA, Watkins SC, Gollin SM, Saunders WS (2004) Resolution of anaphase bridges in cancer cells. *Chromosoma* **112**: 389–397.

Jallepalli PV, Lengauer C (2001) Chromosome segregation and cancer: cutting through the mystery. *Nat Rev Cancer* **1**: 109–117.

Ketel CS, Andersen EF, Vargas ML, Suh J, Strome S, Simon JA (2005) Subunit contributions to histone methyltransferase activities of fly and worm polycomb group complexes. *Mol Cell Biol* **25**: 6857–6868.

Kirmizis A, Bartley SM, Farnham PJ (2003) Identification of the polycomb group protein SU(Z)12 as a potential molecular target for human cancer therapy. *Mol Cancer Ther* **2**: 113–121.

Kirmizis A, Bartley SM, Kuzmichev A *et al.* (2004) Silencing of human polycomb target genes is associated with methylation of histone H3 Lys 27. *Genes Dev* **18**: 1592–1605.

Kuzmichev A, Nishioka K, Erdjument-Bromage H, Tempst P, Reinberg D (2002) Histone methyltransferase activity associated with a human multiprotein complex containing the Enhancer of Zeste protein. *Genes Dev* **16**: 2893–2905.

Kuzmichev A, Jenuwein T, Tempst P, Reinberg D (2004) Different EZH2-containing complexes target methylation of histone H1 or nucleosomal histone H3. *Mol Cell* **14**: 183–193.

Lachner M, O'Carroll D, Rea S, Mechtler K, Jenuwein T (2001) Methylation of histone H3 lysine 9 creates a binding site for HP1 proteins. *Nature* **410**: 116–120.

Lee TI, Jenner RG, Boyer LA, Guenther MG, Levine SS, Kumar RM, Chevalier B, Johnstone SE, Cole MF, Isono K, Koseki H, Fuchikami T, Abe K, Murray HL, Zucker JP, Yuan B, Bell GW, Herbolsheimer E, Hannett NM, Sun K, Odom DT, Otte AP, Volkert TL, Bartel DP, Melton DA, Gifford DK, Jaenisch R, Young RA (2006) Control of developmental regulators by Polycomb in human embryonic stem cells. *Cell* **125**: 301–313.

Lehnertz B, Ueda Y, Derijck AA *et al.* (2003) Suv39h-mediated histone H3 lysine 9 methylation directs DNA methylation to major satellite repeats at pericentric heterochromatin. *Curr Biol* **13**: 1192–1200.

Maison C, Bailly D, Peters AH *et al.* (2002) Higher-order structure in pericentric heterochromatin involves a distinct pattern of histone modification and an RNA component. *Nat Genet* **30**: 329–334.

Melcher M, Schmid M, Aagaard L, Selenko P, Laible G, Jenuwein T (2000) Structure-function analysis of SUV39H1 reveals a dominant role in heterochromatin organization, chromosome segregation, and mitotic progression. *Mol Cell Biol* **20**: 3728–3741.

Minc E, Allory Y, Worman HJ, Courvalin JC, Buendia B (1999) Localization and phosphorylation of HP1 proteins during the cell cycle in mammalian cells. *Chromosoma* **108**: 220–234.

Muller J, Hart CM, Francis NJ *et al.* (2002) Histone methyltransferase activity of a Drosophila Polycomb group repressor complex. *Cell* **111**: 197–208.

Nakayama J, Rice JC, Strahl BD, Allis CD, Grewal SI (2001) Role of histone H3 lysine 9 methylation in epigenetic control of heterochromatin assembly. *Science* **292**: 110–113.

Nekrasov M, Wild B, Muller J (2005) Nucleosome binding and histone methyltransferase activity of Drosophila PRC2. *EMBO Rep* **6**: 348–353.

Nielsen AL, Oulad-Abdelghani M, Ortiz JA, Remboutsika E, Chambon P, Losson R (2001) Heterochromatin formation in mammalian cells: interaction between histones and HP1 proteins. *Mol Cell* **7**: 729–739.

O'Carroll D, Scherthan H, Peters AH *et al.* (2000) Isolation and characterization of Suv39h2, a second histone H3 methyltransferase gene that displays testis-specific expression. *Mol Cell Biol* **20**: 9423–9433.

Pal-Bhadra M, Leibovitch BA, Gandhi SG *et al.* (2004) Heterochromatic silencing and HP1 localization in Drosophila are dependent on the RNAi machinery. *Science* **303**: 669–672.

Pasini D, Bracken AP, Jensen MR, Denchi EL, Helin K (2004) Suz12 is essential for mouse development and for EZH2 histone methyltransferase activity. *Embo J* **23**: 4061–4071.

Peters AH, Kubicek S, Mechtler K *et al.* (2003) Partitioning and plasticity of repressive histone methylation states in mammalian chromatin. *Mol Cell* **12**: 1577–1589.

Peters AH, O'Carroll D, Scherthan H *et al.* (2001) Loss of the Suv39h histone methyltransferases impairs mammalian heterochromatin and genome stability. *Cell* **107**: 323–337.

Plath K, Fang J, Mlynarczyk-Evans SK *et al.* (2003) Role of histone H3 lysine 27 methylation in X inactivation. *Science* **300**: 131–135.

Rea S, Eisenhaber F, O'Carroll D *et al.* (2000) Regulation of chromatin structure by site-specific histone H3 methyltransferases. *Nature* **406**: 593–599.

Reuter G, Wolff I (1981) Isolation of dominant suppressor mutations for position-effect variegation in Drosophila melanogaster. *Mol Gen Genet* **182**: 516–519.

Rice JC, Briggs SD, Ueberheide B *et al.* (2003) Histone methyltransferases direct different degrees of methylation to define distinct chromatin domains. *Mol Cell* **12**: 1591–1598.

Silva J, Mak W, Zvetkova I *et al.* (2003) Establishment of histone h3 methylation on the inactive X chromosome requires transient

recruitment of Eed-Enx1 polycomb group complexes. *Dev Cell* **4**: 481–495.

Sinclair DA, Lloyd VK, Grigliatti TA (1989) Characterization of mutations that enhance position-effect variegation in Drosophila melanogaster. *Mol Gen Genet* **216**: 328–333.

Taddei A, Maison C, Roche D, Almouzni G (2001) Reversible disruption of pericentric heterochromatin and centromere function by inhibiting deacetylases. *Nat Cell Biol* **3**: 114–120.

Tonozuka Y, Minoshima Y, Bao YC *et al.* (2004) A GTPase-activating protein binds STAT3 and is required for IL-6-induced STAT3 activation and for differentiation of a leukemic cell line. *Blood* **104**: 3550–3557.

Yamamoto K, Sonoda M (2003) Self-interaction of heterochromatin protein 1 is required for direct binding to histone methyltransferase, SUV39H1. *Biochem Biophys Res Commun* **301**: 287–292.

Yamamoto K, Sonoda M, Inokuchi J, Shirasawa S, Sasazuki T (2004) Polycomb group suppressor of zeste 12 links heterochromatin protein 1 alpha and enhancer of zeste 2. *J Biol Chem* **279**: 401–406.

THE JOURNAL OF BIOLOGICAL CHEMISTRY VOL. 282, NO. 22, pp. 16391–16400, June 1, 2007

Overlapping Roles of the Methylated DNA-binding Protein MBD1 and Polycomb Group Proteins in Transcriptional Repression of *HOXA* Genes and Heterochromatin Foci Formation*[S]

Received for publication, January 2, 2007, and in revised form, March 22, 2007 Published, JBC Papers in Press, April 11, 2007, DOI 10.1074/jbc.M700011200

Yasuo Sakamoto[‡§1], Sugiko Watanabe[‡], Takaya Ichimura[¶], Michio Kawasuji[‖], Haruhiko Koseki[**], Hideo Baba[§], and Mitsuyoshi Nakao[‡2]

From the [‡]Department of Regeneration Medicine, Institute of Molecular Embryology and Genetics, [§]Department of Gastroenterological Surgery, [¶]Department of Cell Pathology, and [‖]Department of Cardiovascular Surgery, Graduate School of Medical Sciences, Kumamoto University, 2-2-1 Honjo, Kumamoto 860-0811, Japan and [**]RIKEN Research Center for Allergy and Immunology, 1-7-22 Suehiro, Tsurumi-ku, Yokohama 230-0045, Japan

Methylated DNA binding domain (MBD) proteins and Polycomb group (PcG) proteins maintain epigenetic silencing of transcriptional activity. We report that the DNA methylation-mediated repressor MBD1 interacts with Ring1b and hPc2, the major components of Polycomb repressive complex 1. The cysteine-rich *CXXC* domains of MBD1 bound to Ring1b and the chromodomain of hPc2. Chromatin immunoprecipitation analysis revealed that MBD1 and hPc2 were present in silenced Homeobox A (*HOXA*) genes which could be reactivated by knockdown of either MBD1 or hPc2, suggesting that MBD1 and hPc2 cooperate for transcriptional repression of *HOXA* genes. In the nuclei of HeLa cells, MBD1 existed in close association with these PcG proteins in some heterochromatin foci, whereas an MBD1 mutant lacking the *CXXC* domains or an hPc2 mutant lacking the chromodomain lost this colocalization in foci. Use of the DNA demethylating agent 5-azadeoxycytidine abolished the formation of MBD1 foci but not PcG foci. Knockdown of MBD1 by small interfering RNAs did not affect the foci containing hPc2 and Ring1b, whereas the MBD1 foci were not influenced by knockdown of hPc2. These indicate that the heterochromatin foci showing MBD1 and hPc2 colocalization arise through the interaction of MBD1 and hPc2 and that the foci of MBD1 are separable from those of the PcG proteins *per se*. Our present findings suggest that MBD1 and PcG proteins have overlapping roles in epigenetic gene silencing and heterochromatin foci formation through their interactions.

Patterns of gene expression are stably inherited during somatic cell division through maintenance of the epigenetic state of the mammalian genome (1, 2). The two major epigenetic silencing pathways play essential roles in this process as mechanisms of cellular memory. One pathway involves DNA methylation and subsequent recognition by methylated DNA binding domain (MBD)[3] proteins (3–5), whereas the other pathway is a repressive mechanism involving Polycomb group (PcG) protein complexes (6, 7).

Cytosine methylation in 5′-CpG-3′ dinucleotides is well correlated with gene repression and the formation of transcriptionally inactive chromatin (8). DNA methyltransferases (DNMTs) methylate genomic DNAs followed by binding of MBD family proteins (9, 10). To date, five members of the MBD family have been identified in mammals by the presence of highly conserved MBD sequences (3–5). Among these, MBD1 is known to act as a transcriptional repressor through cooperation of the MBD, cysteine-rich *CXXC* domains (*CXXC*1, *CXXC*2, and *CXXC*3), and a transcriptional repression domain (TRD) (11–13). The MBD of MBD1 binds a symmetrically methylated CpG sequence (14) and is also associated with a histone methyltransferase, Suv39h1, which methylates lysine 9 of histone H3 (H3K9) and heterochromatin protein 1 (15). Furthermore, the TRD of MBD1 produces a strong repressive activity by recruiting MBD1-containing chromatin-associated factor 1 (MCAF1)/ATFa-associated modulator (AM) (16, 17). MCAF1/AM complexes with another histone methyltransferase, SETDB1, and is required for trimethylation of H3K9 by this enzyme (18). In addition, there are at least five isoforms of MBD1 that are alternatively spliced in the region containing the three *CXXC* sequences (11). The *CXXC* domain was originally found in DNMT1 and the Trithorax group protein ALL-1 (also known as MLL) (11). Although the *CXXC*3 domain of MBD1 was shown to bind DNA (13, 19), the significance of the *CXXC* domains in MBD1 remains to be determined.

The Polycomb group (PcG) proteins were initially identified as regulators of the *homeobox* (*hox*) genes during development

* This work was supported by a grant-in-aid for Scientific Research on Priority Areas, a grant-in-aid for 21st Century COE (Center of Excellence) Research from the Ministry of Education, Culture, Sports, Science, and Technology, and a research grant from the Takeda Science Foundation (to M. N.). The costs of publication of this article were defrayed in part by the payment of page charges. This article must therefore be hereby marked "*advertisement*" in accordance with 18 U.S.C. Section 1734 solely to indicate this fact.

[S] The on-line version of this article (available at http://www.jbc.org) contains supplemental Figs. 1–4 and Tables 1 and 2.

[1] A COE Junior Research Associate.

[2] To whom correspondence should be addressed. Tel.: 81-96-373-6800; Fax: 81-96-373-6804; E-mail: mnakao@gpo.kumamoto-u.ac.jp.

[3] The abbreviations used are: MBD, methylated DNA binding domain; PcG, Polycomb group; TRD, transcriptional repression domain; H3K9, lysine 9 of histone H3; PRC, Polycomb repressive complexes; RT, reverse transcription; NLS, nuclear localization signal; DNMT, DNA methyltransferase; siRNA, small interfering RNA; GST, glutathione S-transferase; GFP, green fluorescent protein.

in *Drosophila melanogaster* (20). These proteins are evolutionarily conserved in mammals and are expected to maintain the heritable repressive state of the *HOX* genes and various growth-controlling genes (21, 22). Similarly to the DNA methylation system, PcG proteins are involved in a variety of phenomena, such as X-chromosome inactivation, genomic imprinting, and control of cell proliferation and differentiation (23–25). Biochemical and genetic studies have indicated that PcG proteins can be classified into at least two Polycomb repressive complexes (PRC) named PRC1 and PRC2 (25–27). At the initiation of gene silencing, PRC2, which contains EED, EZH2, YY1, and SU(Z)12, is recruited to methylate lysine 27 of histone H3 (H3K27) via the histone methyltransferase EZH2 present in the complex. At the maintenance stage, PRC1, which contains Ring1b, hPc2, and BMI1, binds the trimethylated H3K27 through recognition by hPc2 (28, 29). The sequential actions of these PRCs result in stable maintenance of gene silencing. It is of interest that EZH2 and BMI1 are overexpressed in certain cancers and have been implicated in the process of tumorigenesis (30), suggesting that PcG proteins are crucial for cell regulation.

Despite the biological importance of MBD proteins and PcG proteins, the functional relationship of these repressive proteins has remained unknown. A recent study showed that EZH2 in PRC2 directly interacts with DNMTs and maintains CpG methylation at EZH2-targeted promoters (31), suggesting that EZH2 directly controls DNA methylation of EZH2 target genes. Mice embryos deficient for *Eed* changed the DNA methylation status of specific CpGs in differentially methylated regions at imprinted loci (32). As well, the association of BMI1 with PcG bodies, sites of the PcG complex accumulation mostly located in heterochromatin regions, requires DNMT1 as well as EZH2 and EED (33). This suggests that DNMT1 is involved in the formation of silent chromatin by PcG proteins. Collectively, these observations suggest that the two epigenetic silencing pathways are mechanistically linked. During an investigation of the roles of the CXXC domains of MBD1, we found that MBD1 interacts with Ring1b and hPc2, which are key molecules in PRC1. Here, we present evidence demonstrating the importance of the overlapping roles of MBD1 and PcG proteins in transcriptional repression of *HOXA* genes and heterochromatin foci formation.

EXPERIMENTAL PROCEDURES

Yeast Two-hybrid Screening—Yeast strain AH109 carrying pAS2-1-CXXC domain of MBD1 (amino acids 150–268 in isoform v1) was transformed with the mouse E17 whole embryo cDNA libraries constructed in pACT2 (Clontech). Plasmids harboring cDNA were recovered from both histidine- and adenine-positive colonies and were used for DNA sequencing analysis.

Plasmids—The cDNA for hPc2 and Ring1b were cloned into pcDNA3 (pcDNA3-FLAG-hPc2 and pcDNA3-DsRed-monomer-Ring1b). The chromodomain of hPc2 (amino acids 3–71) was subcloned into pCMV-GAL4. pSilencer3.1puro vector (Ambion) was used to express small hairpin RNAs. Target sequences are indicated in supplemental Table 1. The pCGN-MBD1, pEGFP-MBD1, and pCMV-GAL4-CXXC of MBD1 were previously described (13).

Cell Culture—HeLa cells were cultured in a 1:1 mixture of Dulbecco's modified Eagle's minimum essential medium and Ham's F-12 nutrient medium (Sigma) supplied with 10% (v/v) heat-inactivated fetal bovine serum.

Transfection and Cell Treatment—HeLa cells were transfected with plasmid DNAs by using a liposome-mediated gene transfer method. For the luciferase assay, HeLa cells (1.0×10^5 cells) were transfected with siRNA expression vector (2.0 μg) with FuGene6 (Roche Applied Science) in a 6-well plate, and after 24 h the cells were diluted to 1:2 and transferred to a 12-well plate under selection with puromycin (1.0 μg/ml). In addition, HeLa cells were treated with 5 μM 5-aza-2-deoxycytidine. After 3 days, the treated cells were used for immunofluorescent assay and reverse transcription (RT)-PCR.

Protein Expression—The cDNAs for Ring1b, hPc2, and the deletion mutants of hPc2 were cloned into pET28a (Novagen). The expression of these proteins, GST-fused MBD1v1 and GST-fused portions of MBD1, were performed as described previously (17).

Antibodies—The polyclonal antibodies against hPc2 were generated by immunizing a rabbit against His-tagged hPc2 (amino acids 59–466). For affinity purification of the antibodies, His-tagged hPc2 (amino acids 59–466) was coupled to HiTrap Protein G HP (GE Healthcare). Rabbit anti-MBD1 polyclonal antibodies were previously described (13). Mouse anti-Ring1b monoclonal antibodies were provided from Dr. H. Koseki. Other antibodies utilized were anti-MBD1 (Santa Cruz), anti-trimethylated H3K9, anti-trimethylated H3K27 (Upstate), anti-FLAG (M5) (Sigma), anti-His tag (Qiagen), anti-GST (DAKO), anti-lamin A/C (Santa Cruz), anti-GAL4 (Santa Cruz), and anti-β-tubulin (Amersham Biosciences).

Immunoprecipitation—HeLa cells were treated with dimethyl 3,3′-dithiobispropionimidate-2HCl (5 mM) (Pierce) in phosphate-buffered saline, rinsed with an ice-cold buffer (100 mM Tris-HCl (pH 8.0), 150 mM NaCl), and lysed with a hypotonic buffer (10 mM Tris-HCl (pH 7.9), 10 mM NaCl, 1.5 mM $MgCl_2$) supplemented with protease inhibitors for 10 min at 4 °C. The nuclei were collected by centrifugation (1500 rpm) at 4 °C for 10 min, mixed with buffer containing 20 mM Tris-HCl (pH 7.9), 420 mM NaCl, 25% glycerol, 1.5 mM $MgCl_2$, 0.2 mM EDTA, and protease inhibitors, and then incubated with rotation for 30 min at 4 °C. After centrifugation (1500 rpm), the nuclei extracts were lysed using sonication with a radioimmune precipitation assay buffer (1% Nonidet P-40, 0.1% SDS, 500 mM NaCl, 50 mM Tris-HCl (pH 7.4), 5 mM EDTA, 5% glycerol, 1% sodium deoxycholate, and protease inhibitors). The lysates were incubated for 1 h at 4 °C with specific antibodies or control IgG and then incubated for 1 h after the addition of 20 μl of protein A/G-agarose beads (Amersham Biosciences). After the washings, the bound proteins were detected by Western blot analysis.

In Vitro Binding and GST Pulldown Assay—Bacterially expressed GST and GST fusion proteins (1 μg) were immobilized on glutathione-agarose beads and incubated with His-tagged PcG proteins (1 μg) in a buffer containing 0.05% Triton X-100, 50 mM HEPES (pH 7.4), 150 mM NaCl, 5% glycerol, 10

μM $ZnCl_2$, 1 mM dithiothreitol, and protease inhibitors for 1 h at 4 °C. The input indicates 10% of the His-tagged proteins.

Immunofluorescent Analysis—After being washed 2 times with phosphate-buffered saline (PBS), HeLa cells were similarly fixed 4% paraformaldehyde in PBS for 15 min at room temperature and then treated with 0.2% Triton X-100 for 5 min at 4 °C. After washing the cells with phosphate-buffered saline (PBS) containing 0.5% bovine serum albumin, we incubated them with specific antibodies in PBS containing 0.2% bovine serum albumin for 1 h at room temperature. Samples were analyzed with an Olympus IX71 microscope using LuminaVision software.

Luciferase Assay—At 48 h after transfection with a luciferase reporter plasmid and together with pCMV-GAL4 (*CXXC* domains of MBD1 or chromodomain of hPc2) and pcDNA3-FLAG-hPc2, HeLa cells were lysed in a buffer provided by the manufacturer (Promega). pRL-SV40, insertless pcDNA3, and pCMV-GAL4 were used as controls. Values are the means and S.D. of results from three independent experiments.

Chromatin Immunoprecipitation—HeLa cells (1×10^6) were treated with dimethyl 3,3′-dithiobispropionimidate-2HCl (5 mM), rinsed, and then cross-linked by the addition of 1% formaldehyde at 37 °C for 10 min. Crude cell lysates were sonicated to generate 200–1000 bp of DNA fragments. Chromatin immunoprecipitation was performed with anti-MBD1, anti-hPc2 antibodies, or control IgG according to the manufacturer's protocols (Upstate Biotechnology, Inc.). PCR amplification of human *HOXA* gene promoters was carried out for 35 cycles under the conditions of 30 s at 94 °C, 30 s at 56 °C, and 30 s at 72 °C using specific set of primers described in supplemental Table 2. DNAs in input lysates were used as a positive control (input control).

siRNA Knockdown of MBD1 and hPc2—Twenty-one-nucleotide siRNA duplexes were designed to target mRNAs encoding human MBD1 and hPc2. The selected siRNA target sequences were submitted to human genome and EST databases to ensure the target specificities. These sequences were described in supplemental Table 1. The siRNAs for lamin A/C were previously reported (17). The siRNAs were transfected into the cells using Oligofectamine (Invitrogen) for 48 h.

RT-PCR and Quantitative Real-time RT-PCR—Total RNAs were isolated using Isogen (Nippon Gene). For cDNA synthesis, 5 μg of total RNAs was reverse-transcribed with Superscript III (Invitrogen) using oligo-dT or random oligo primers. The RT-PCR was carried out for 30 cycles. Quantitative real-time PCR of the target cDNAs was performed by the SYBR Green method using Power SYBR Green PCR Master Mix (Applied Biosystems). Each experiment was carried out at least three times. The -fold relative enrichment was quantified together with normalization by the β-actin level. The primer sets are listed in supplemental Table 2.

Bisulfite Genomic Sequencing—Genomic DNAs were treated with sodium bisulfite followed by PCR amplification with specific primers using AmpliTaq Gold (Applied Biosystems). The primers used were described in supplemental Table 2. The resulting PCR products were purified and directly sequenced.

RESULTS

MBD1 Interacts with PcG Proteins—To identify factors that interact with MBD1, we performed yeast two-hybrid screening using the region containing the *CXXC* domains (amino acids 150–268) as bait (Fig. 1*A*). From a screening of ~7×10^6 independent transformants of 17-day-old mouse embryo cDNA libraries, we isolated a cDNA clone encoding Ring1b (amino acids 250–337). To confirm an interaction between MBD1 and Ring1b, we prepared His-tagged full-length Ring1b and subjected it to an *in vitro* pulldown analysis (Fig. 1*B*). Briefly, GST and GST-fused portions of MBD1 were immobilized on glutathione-agarose beads and incubated with His-Ring1b. Ring1b predominantly bound the *CXXC*1 and *CXXC*2 domains of MBD1, but not its MBD, *CXXC*3, and TRD domains, in agreement with the yeast two-hybrid screen.

Our previous alignment analysis revealed that the amino acid sequence of the *CXXC*3 domain of MBD1 shows high identity with that of the *CXXC* domain of ALL1/MLL (11). ALL1/MLL is one of the Trithorax group proteins and methylates histone H3 at lysine 4 (34, 35). It was previously reported that the region containing the *CXXC* domain of ALL1/MLL interacts with hPc2 (36). To test whether the *CXXC* domains of MBD1 can interact with hPc2, His-tagged hPc2 was prepared for an *in vitro* pulldown analysis (Fig. 1*B*). His-hPc2 specifically bound the *CXXC*3 domain as well as full-length MBD1. To further determine the region responsible for binding MBD1, we used two deletion mutants of hPc2, hPc2ΔN, and hPc2ΔC, which lacked the amino- and carboxyl-terminal regions of the protein, respectively (Fig. 1*A*). hPc2ΔC bound GST-MBD1, whereas hPc2ΔN lacking the chromodomain did not (Fig. 1*C*). These data suggest that the *CXXC* domains of MBD1 directly interact with Ring1b and hPc2, which are essential components of PRC1.

MBD1 Forms Complexes with PcG Proteins in Vivo—To confirm the interactions between MBD1 and PcG proteins *in vivo*, we performed an immunoprecipitation analysis. Hemagglutinin-tagged MBD1 and FLAG-tagged hPc2 were coexpressed in HeLa cells and immunoprecipitated by anti-MBD1 and anti-hPc2 antibodies, respectively. Western blot analysis revealed that MBD1 was present in the immunoprecipitates with hPc2 but not in control immunoprecipitates (Fig. 1*D*). hPc2 was detected in the immunoprecipitates with MBD1. Likewise, an immunoprecipitation analysis after coexpression of hemagglutinin-MBD1 and DsRed-tagged Ring1b revealed that MBD1 formed complexes with Ring1b (data not shown). To confirm whether exogenously expressed hPc2 and Ring1b form complexes in cells, immunoprecipitation of FLAG-hPc2 and DsRed-Ring1b was carried out (Fig. 1*E*). These PcG proteins were found to be mutually coprecipitated. We further investigated the association of endogenous MBD1 and hPc2 in HeLa cells without any overexpression. The coprecipitated bands for endogenous proteins were relatively faint and constant in repeated experiments (data not shown), probably due to the low biochemical solubility of endogenous MBD1 (16, 37). Together with the colocalization data (see Figs. 4 and 5), these results show that MBD1 and PcG proteins form complexes *in vivo*.

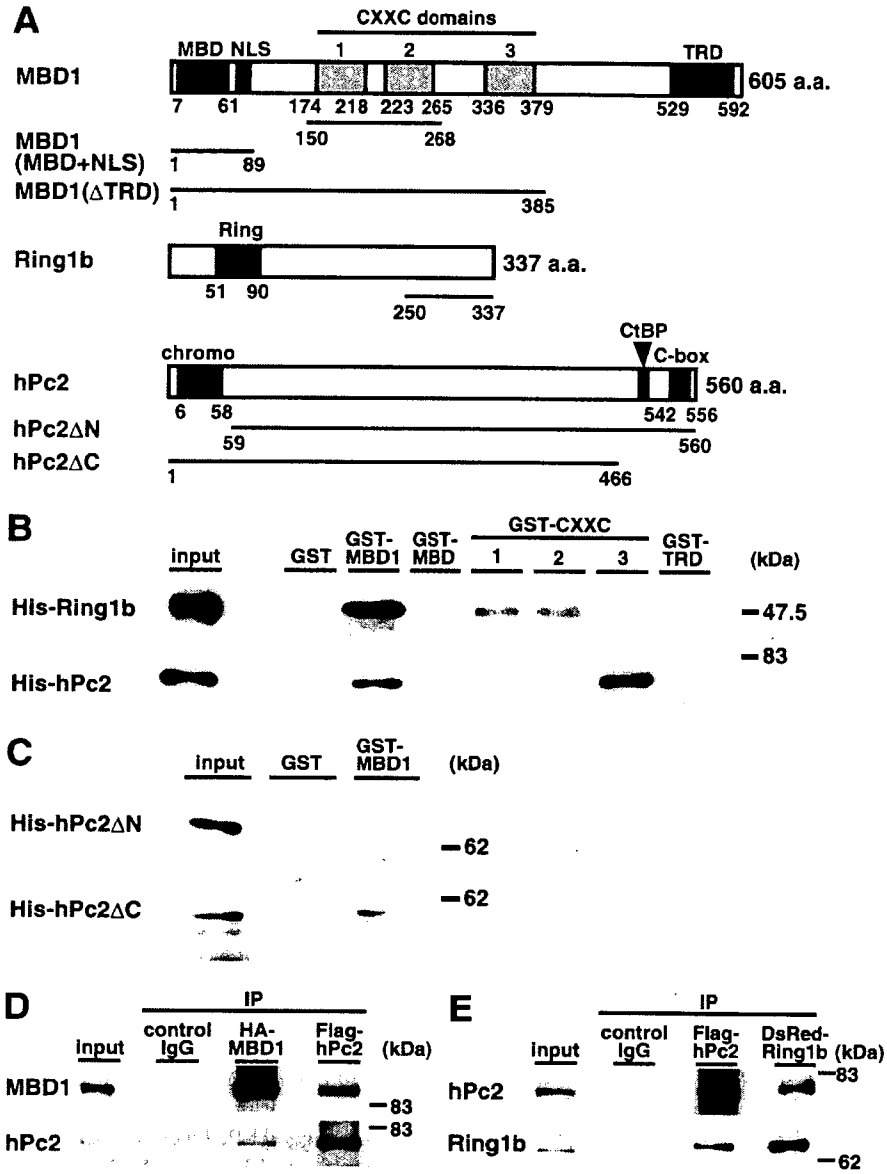

FIGURE 1. **Interaction of MBD1 with PcG proteins.** *A*, structures of MBD1, Ring1b, and hPc2. MBD1 contains a MBD, NLS, cysteine-rich *CXXC* domains, and TRD. The *CXXC* 1 and 2 domains (amino acids 150–268) were used as bait in a yeast two-hybrid screen, resulting in the identification of Ring1b (amino acids 250–337). Ring1b contains a Ring domain, whereas hPc2 contains a chromodomain, CtBP binding domain, and C-box. Deletion mutants of MBD1 and hPc2 are also shown. *a.a.*, amino acids. *B*, direct binding of Ring1b and hPc2 to MBD1. Recombinant GST and GST-fused MBD1 and individual domains (MBD, *CXXC*1, *CXXC*2, *CXXC*3, and TRD) were incubated with His_6-fused Ring1b or hPc2. Western blot analysis was performed with anti-His antibodies. *C*, interaction of the chromodomain of hPc2 with MBD1. The deletion mutants of hPc2 were used for GST pulldown assays. The input shows 10% of each protein. *D*, complex formation of MBD1 and hPc2. *E*, complex formation of hPc2 and Ring1b. Hemagglutinin (*HA*)-tagged MBD1, FLAG-tagged hPc2, and DsRed-Ring1b were expressed in HeLa cells. Western blot analysis of immunoprecipitates (*IP*) was performed with anti-MBD1, anti-hPc2, and anti-Ring1b antibodies. The input shows 10% of each lysate.

Cooperative Interaction of MBD1 and hPc2 for a Transcriptional Role—We tested whether combinations of the *CXXC* domains of MBD1 and hPc2 and of the chromodomain of hPc2 and MBD1 functionally interact for transcriptional control using luciferase reporter experiments (Fig. 2*A*). We expressed GAL4-fused *CXXC* domains of MBD1 (GAL4-*CXXC*) or the GAL4-fused chromodomain of hPc2 (GAL4-chromo) in HeLa cells. Western blot analyses revealed that GAL4-*CXXC* and GAL4-chromo were appropriately expressed in this assay (Fig. 2, *B–D*). The effects of the combinations were examined by using a *Photinus pyralis* luciferase reporter containing five GAL4 binding elements upstream of the human *p16* gene promoter. The *p16* gene is targeted by CpG hypermethylation and subsequent binding of MBD1 or by PcG proteins in certain cancer cells (10, 30, 38, 39). GAL4-*CXXC* alone tended to decrease the luciferase activity in a dose-dependent manner (Fig. 2*B*). To assess the functional implication of the MBD1-hPc2 association, we checked the effect of exogenous hPc2 on the *CXXC*-based transcription. Coexpression of FLAG-hPc2 moderately decreased the *CXXC*-based luciferase activities, consistent with the interaction of MBD1 with hPc2. To elucidate the cooperative role of MBD1 and hPc2, we performed selective knockdown of endogenous hPc2 or MBD1 using pSilencer3.1puro vectors producing specific short hairpin RNAs (Fig. 2*C*). Western blot analyses revealed the effectiveness of the MBD1 or hPc2 knockdown (supplemental Fig. 1*A*). Knockdown of hPc2 constantly increased the *CXXC*-based transcription compared with the level with *CXXC* alone.

To further examine the transcriptional effect of the chromodomain of hPc2, we expressed GAL4-chromo in HeLa cells (Fig. 2*D*). GAL4-chromo alone efficiently repressed transcription in a dose-dependent manner. To confirm the functional association of MBD1-hPc2, we knocked down endogenous MBD1. In comparison to the controls, the repression of the promoter activities by GAL4-chromo was weakened after knockdown of MBD1. In addition, the expression of GAL4-fused full-length MBD1 or hPc2 alone showed stronger repression of the promoter activity (data not shown). Collectively, these data suggest that the *CXXC* domains of MBD1 associate with the chromodomain of hPc2.

Transcriptional Repression of HOXA Genes by MBD1 and PcG Proteins—There is a possibility that DNA methylation as well as PcG complexes is involved in the repression of *HOX* genes in mammals (40, 41), although the roles of the MBD family proteins have not been investigated. To test the roles of

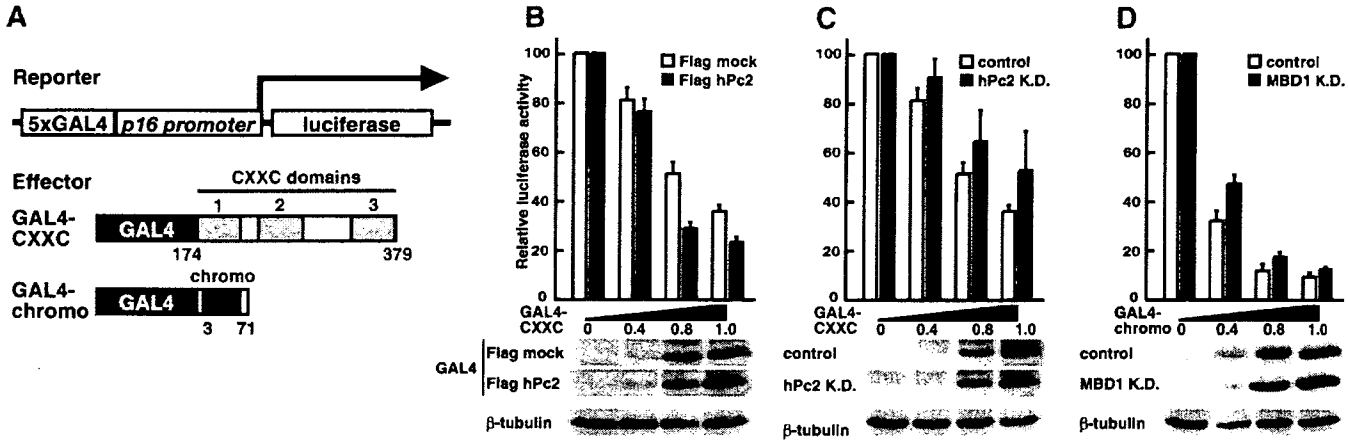

FIGURE 2. **Cooperative interaction of MBD1 and hPc2 for a transcriptional role.** *A*, luciferase reporter assays. GAL4-fused CXXC domains of MBD1 (GAL4-CXXC) and GAL4-fused chromodomain of hPc2 (GAL4-chromo) are shown. The effect of the combinations was examined by using a luciferase reporter containing five GAL4 binding elements upstream of the human *p16* gene promoter. *B*, effect of hPc2 on CXXC domains-based transcription. *C*, effect of hPc2 knockdown (*K.D.*) on CXXC domains-based transcription. *D*, effect of MBD1 knockdown on chromodomain-based transcription. pSilencer-hPc2 and pSilencer-MBD1 were used for the specific knockdowns. The luciferase activities from insertless GAL4-mock were normalized to 100. The levels of expression of the GAL4-fused proteins were not affected by experimental conditions.

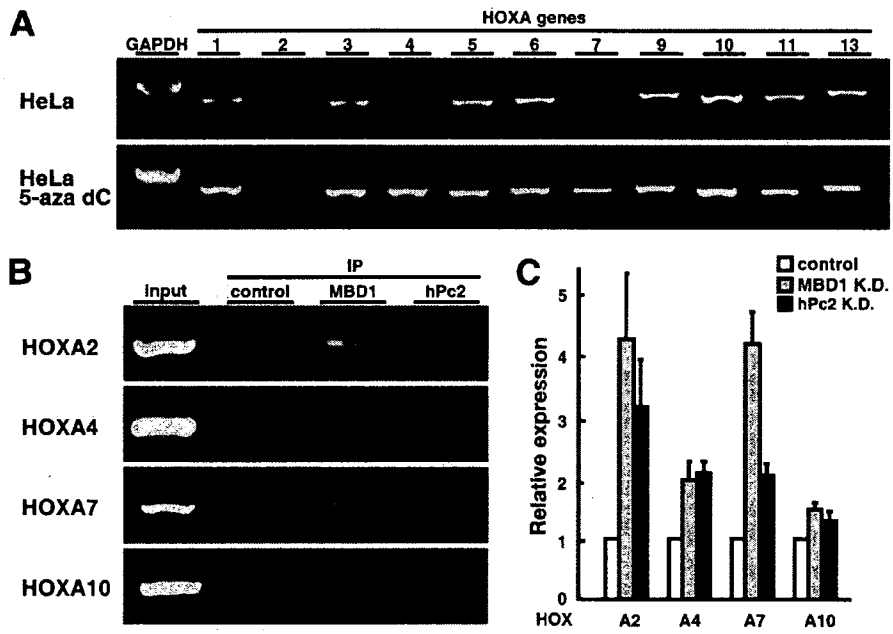

FIGURE 3. **Transcriptional repression of *HOXA* genes by MBD1 and PcG proteins.** *A*, expression status of the *HOXA* gene cluster in HeLa cells. HeLa cells were cultured in the presence of 5 μM 5-aza-dC for 3 days. RT-PCR was carried out using glyceraldehyde-3-phosphate dehydrogenase (*GAPDH*) as a control. *B*, existence of MBD1 and hPc2 in the *HOXA* gene promoters. The *arrows* in supplemental Fig. 3 indicate the primers used for the chromatin immunoprecipitation (*IP*) analysis. *C*, reactivation of silent *HOXA* genes by knockdown (*K.D.*) of MBD1 or hPc2. siRNAs targeting the mRNAs encoding human MBD1 or hPc2 were transfected into the cells. A quantitative real-time PCR analysis was carried out.

MBD1 and PcG proteins in gene regulation, we performed an expression analysis of the *HOXA* gene cluster on human chromosome 7p15.3 using a reverse transcription-PCR method (Fig. 3*A*). The *HOXA2*, *HOXA4*, and *HOXA7* genes were repressed in HeLa cells, whereas other *HOXA* genes were expressed in the cells. The expression profiles of the *HOXA* genes differed among the cell lines tested (supplemental Fig. 2). To check whether the repression was related to DNA methylation, the cells were treated with 5-aza-2-deoxycytidine (5-aza-dC; 5 μM) for 3 days. Under these hypomethylation conditions, the *HOXA4* and *HOXA7* genes were reactivated mostly to the expression levels of the originally transcribed *HOXA* genes. By contrast, the *HOXA2* gene seemed to be relatively resistant to derepression. Next, we focused on characterizing the *HOXA2*, *HOXA4*, *HOXA7*, and *HOXA10* genes. To test the methylation status of these *HOXA* gene promoters, we performed a bisulfite-based genome sequencing analysis (supplemental Fig. 3). The promoter regions of the *HOXA2*, *HOXA4*, and *HOXA7* genes were highly methylated. Unexpectedly, the *HOXA10* promoter was also methylated regardless of the expression state.

To check the existence of MBD1 and hPc2 in these promoters, we performed chromatin immunoprecipitation assays in HeLa cells. After formaldehyde-based cross-linking of proteins and DNAs, fragmented chromatin fractions were immunoprecipitated with anti-MBD1 or anti-hPc2 antibodies followed by PCR amplification using specific primers for the *HOXA* promoters (Fig. 3*B*). Both MBD1 and hPc2 were predominantly present in the *HOXA2* promoter, whereas MBD1 was found in the *HOXA4* and *HOXA7* promoters. By contrast, neither MBD1 nor hPc2 was detected in the *HOXA10* promoter. Last, we studied whether MBD1 and hPc2 were involved in the *HOXA* gene silencing (Fig. 3C). A quantitative real-time PCR analysis was performed to test the transcripts from the *HOXA2*, *HOXA4*, *HOXA7*, and *HOXA10* genes. Compared with the controls, the levels of *HOXA2* mRNA were mark-

edly elevated by more than 3-fold after knockdown of MBD1 or hPc2. Similarly, knockdown of each protein resulted in increased levels of *HOXA4* mRNA (about 2-fold) and *HOXA7* mRNA (about 2–3-fold). Thus, MBD1 and hPc2 are involved in maintaining the repression of these genes. Double knockdown of both proteins did not appear to have an additional derepressive effect (data not shown). By contrast, the expression of *HOXA10* did not change after knockdown of either protein. Collectively, MBD1 and hPc2 have an overlapping role in repression of the *HOXA* genes, and both proteins are required for maintaining the repressed state of the *HOX* genes.

Close Association of MBD1 and PcG Proteins in Heterochromatin Foci—To investigate the localization of MBD1 and PcG proteins in the nuclei, GFP-fused MBD1, FLAG-hPc2 and DsRed-Ring1b were expressed in HeLa cells for immunofluorescence analyses (Fig. 4*A*). GFP-fused MBD1 showed the formation of multiple foci in the nuclei, which were previously reported to include 4′,6-diamidino-2-phenylindole-stained heterochromatin and regions of pericentric heterochromatin in HeLa cells (11, 15). Expression of FLAG-hPc2 produced similar nuclear foci, and both MBD1 and hPc2 were colocalized at some foci (as indicated by *arrowheads*). In addition, hPc2 coexisted with Ring1b at most foci, suggesting the existence of MBD1 and PcG proteins at a part of the heterochromatin foci.

To test the localization of MBD1 deletion mutants relative to hPc2, we expressed MBD1(ΔTRD) and MBD1(MBD+ nuclear localization signal (NLS)), which are shown in Fig. 1*A* together with FLAG-hPc2 (Fig. 4*B*). MBD1(ΔTRD) lacking the TRD preserved the coexistence with hPc2 at the foci. By contrast, MBD1(MBD+NLS) lacking the CXXC domains as well as the TRD formed multiple foci that were distinct from the hPc2 foci. Thus, MBD1(MBD+NLS), which is only able to bind methylated DNAs (11), lost its colocalization with hPc2.

To further check the localization of hPc2 mutants relative to MBD1, we expressed GFP-MBD1 in combination with hPc2ΔN or hPc2ΔC (shown in Fig. 1*A*) (Fig. 4*C*). hPc2ΔN lacking the chromodomain did not bind MBD1 (Fig. 1*C*), whereas hPc2ΔC was reported to lose the ability to form PRC1 complexes due to the absence of CtBP binding and a C-box (42, 43). hPc2ΔN showed multiple nuclear foci, but they were not colocalized with any MBD1 foci, in agreement with the data in Fig. 1*C*. These observations suggest that MBD1 foci are closely localized with PcG foci through the MBD1-hPc2 association. On the other hand, hPc2ΔC containing the chromodomain was unexpectedly found to be diffuse in the nuclei and lose the foci formation, suggesting that concentration of hPc2 in the foci requires the formation of PcG complexes. Taken together, our data suggest that MBD1 and PcG proteins closely exist in some heterochromatin foci through interactions between the CXXC domains and chromodomain of these proteins, respectively.

Cooperative Formation of Heterochromatin Foci by MBD1 and PcG Proteins—We then examined the localizations of endogenous MBD1 and PcG proteins in HeLa cells by immunofluorescence analysis with specific antibodies (Fig. 5*A*).

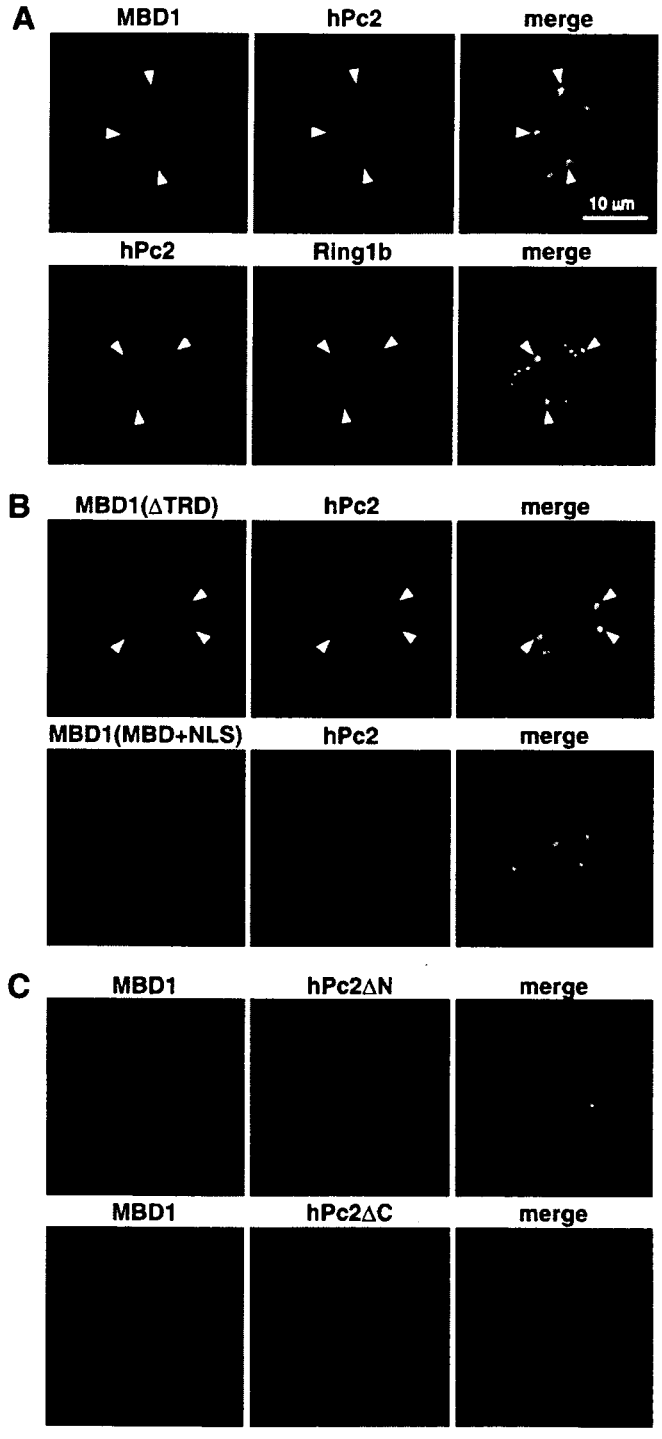

FIGURE 4. **Close association of MBD1 and PcG proteins in heterochromatin foci.** *A*, coexistence of MBD1, hPc2, and Ring1b in heterochromatin foci. GFP-fused MBD1, FLAG-tagged hPc2, and DsRed-Ring1b were expressed in HeLa cells. The *arrowheads* indicate the foci showing colocalization. *B*, effects of MBD1 mutants on the foci showing colocalization. MBD1(MBD + NLS) lacking the CXXC domains loses the colocalization with hPc2 foci. *C*, effects of hPc2 mutants on the foci showing colocalization. hPc2ΔN or hPc2ΔC each lose the colocalization with MBD1 foci.

Similar to the findings in Fig. 4, MBD1 showed multiple foci formation in the nuclei, and some foci were costained with hPc2 and Ring1b. Based on quantitative analyses of 300 foci, 60.1 and 72.7% of MBD1-containing foci coexisted with hPc2

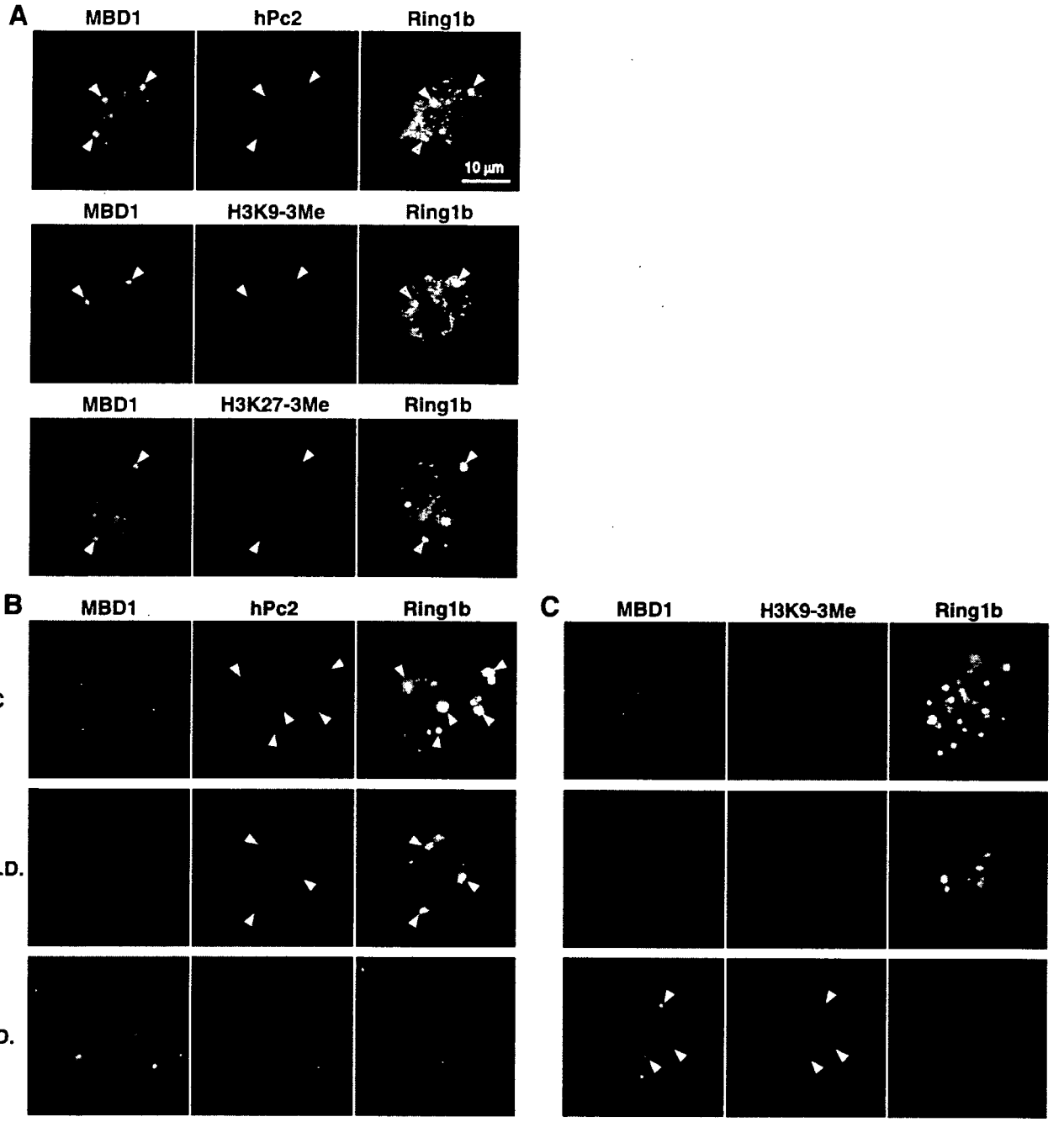

FIGURE 5. **Cooperative formation of heterochromatin foci by MBD1 and PcG proteins.** *A*, colocalization of endogenous MBD1, hPc2, and trimethylation of H3K9 and H3K27 in chromatin foci. The *arrowheads* indicate foci showing colocalization. *B* and *C*, effects of DNA hypomethylation and knockdown (*K.D.*) of MBD1 or hPc2 on the foci showing colocalization. The cells were grown in the presence of 5 μM 5-aza-dC for 3 days or transfected with specific siRNAs targeted against the mRNAs encoding human MBD1 or hPc2. Quantitative analyses of each 300 foci were performed to examine the levels of the colocalization.

and Ring1b, respectively. In addition, 78.7% of hPc2-containing foci were colocalized with Ring1b. To characterize the heterochromatin foci targeted by both MBD1 and PcG proteins, we tested modifications of histone H3 using rabbit anti-trimethyl H3K9 (H3K9-3Me) and anti-trimethyl H3K27 (H3K27-3Me) polyclonal antibodies (44). MBD1 recruits H3K9 methyltransferases to CpG-methylated genomic regions (15, 17, 45). On the other hand, PRC1 complexes are localized to methyl H3K27-marked chromatin via hPc2 (28, 29). As shown in Fig. 5*A*, the heterochromatin foci in which MBD1 and Ring1b coexisted were stained with the trimethyl H3K9 and H3K27. About 74.7 and 27.3% of MBD1 foci appeared to be marked with H3K9-3Me and H3K27-3Me, respectively. The observations suggest that distinct types of chromatin foci, namely MBD1 foci and PcG foci, are structurally overlaid in the nuclei.

To clarify whether or not the formations of these two foci are dependent on each other *in vivo*, we investigated the localizations of these proteins under conditions of DNA hypomethylation (Figs. 5, *B* and *C*). The cells were cultured

in the presence of the DNA demethylating agent 5-aza-dC (5 μM) for 3 days. The treatment was effective for inducing DNA hypomethylation of the genome (data not shown). The use of 5-aza-dC abolished the formation of MBD1 foci marked by trimethyl H3K9, but not the foci containing hPc2 and Ring1b (*upper panels*). Interestingly, the number of PcG foci tended to increase 3–4-fold under conditions of DNA hypomethylation. Western blot analysis revealed that the expression levels of MBD1 and hPc2 proteins did not change in the 5-aza-dC-treated cells (supplemental Fig. 4). Next, we performed specific small interfering RNA-mediated knockdown of endogenous MBD1 or hPc2 (supplemental Fig. 1*B*). In the MBD1 knockdown cells, there were no foci marked by trimethyl H3K9 as well as MBD1 (Fig. 5, *B* and *C*, *middle panels*). By contrast, the foci containing hPc2 and Ring1b were not affected by knockdown of MBD1. Under the MBD1-depleted condition, the colocalization of Ring1b-containing foci with the trimethyl H3K27 did not significantly change (data not shown). Furthermore, knockdown of hPc2 disturbed the PcG foci detected by both hPc2 and Ring1b, whereas MBD1 and trimethyl H3K9 were found to form foci (Fig. 5, *B* and *C*, *lower panels*). Under the hPc2 knockdown, the colocalization of MBD1 foci with trimethyl H3K27 appeared to decrease to 10.0%, suggesting that hPc2 is involved in the colocalization of MBD1 foci and PcG foci. These data indicate that the heterochromatin foci containing MBD1 are separable from those containing PcG proteins *per se*. In addition, our data emphasize that MBD1 coexists with DNA methylation and trimethyl H3K9 (17, 18). As shown in Fig. 4, some of these foci appeared to be closely overlaid in the nuclei through the interaction between MBD1 and hPc2.

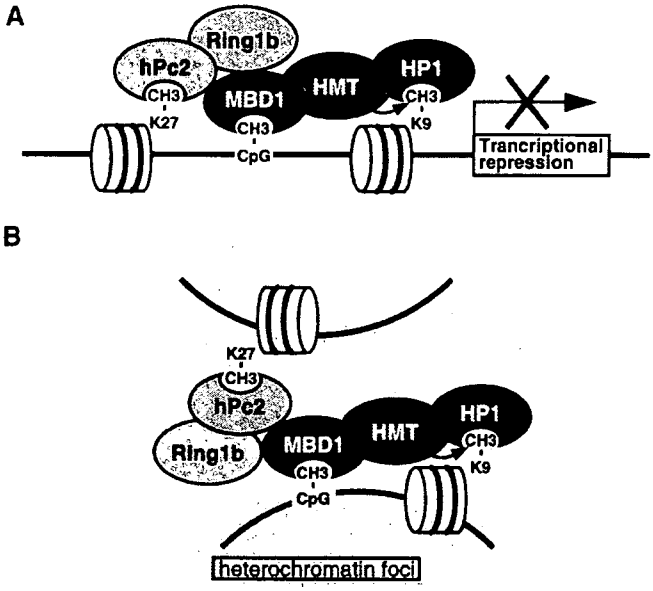

FIGURE 6. **Model for overlapping roles of MBD1 and Polycomb group proteins.** *A*, model of transcriptional repression. MBD1 and Polycomb group proteins including hPc2 and Ring1b have distinct scaffolds and overlapping roles to repress transcription of target genes such as *HOXA* genes. MBD1 recruits H3K9-methytransferase complexes SETDB1-MBD1-containing chromatin-associated factor-AM to form heterochromatin (17). *B*, model of heterochromatin foci formation. Polycomb group proteins form heterochromatin on methylated H3K27-marked regions, whereas MBD1 and H3K9-methytransferase complexes form heterochromatin on CpG-methylated DNA regions. These two heterochromatin regions are colocalized and overlaid by interaction of MBD1 and Polycomb group proteins.

DISCUSSION

Mechanism of Heritable Gene Repression by MBD1 and PcG Proteins—In the present study we found that MBD1 interacts with Ring1b and hPc2, which are essential components of the maintenance PcG complex (PRC1). The overlapping roles of these proteins contribute to the transcriptional gene silencing and maintenance of heterochromatin foci formation, providing the first evidence of cooperation between MBD proteins and PcG proteins. In DNA methylation-mediated repression, MBD1 binds methyl-CpG pairs that are modified with DNMTs and recruits H3K9-specific histone methyltransferases, resulting in subsequent accumulation of heterochromatin protein 1 in the CpG-methylated regions (5, 15, 17, 45). On the other hand, EZH2 in the initiation complex (PRC2) methylates H3K27, which is then recognized by hPc2 and the other components of PRC1 for PcG-mediated repression (25–27). Thus, there are mechanistic similarities in the two major repressive pathways, especially through the involvement of both histone methylation and chromodomain proteins such as heterochromatin protein 1 and hPc2. Importantly, our knockdown of MBD1 or hPc2 revealed that these pathways cooperate in both gene silencing and heterochromatin foci formation. The model for overlapping roles of MBD1 and Polycomb group proteins in epigenetic regulation is proposed in Fig. 6. It was recently reported that EZH2 directly interacts with DNMTs to maintain CpG methylation of the EZH2 target genes (31) and that the association of BMI1 with PcG bodies requires DNMT1 (33). These findings suggest that DNMTs are associated with PRC2 and PRC1. Furthermore, the cooperation of MBD1 and the PRC1 proteins collectively emphasizes that the DNA methylation system is directly linked to the PcG system in mammals. Especially, our data revealed that both MBD1 and PRC1 proteins such as hPc2 are required for maintenance of stable repression of *HOXA* genes and the heterochromatin foci, suggesting their overlapping roles in epigenetic regulation. In addition, MBD1 is known to have at least five isoforms, which are alternatively spliced in the region containing the *CXXC* domains (11). Although the significance of the *CXXC* domains has remained unclear, our data that MBD1 interacts with Ring1b via *CXXC*1 and *CXXC*2 and with hPc2 via *CXXC*3 suggest that the MBD1 isoforms have distinct roles via interactions with the associated proteins. On the other hand, the chromodomain of hPc2 binds not only methyl-H3K27 but also the *CXXC* domain of MBD1 and ALL1/MLL, suggesting a new localization mechanism for the PcG proteins.

Transcriptional Control of HOXA Genes by MBD1 and PcG Proteins—We investigated the repressive roles of MBD1 and hPc2 at the *HOXA* gene cluster targeted by the PcG proteins and DNA methylation. Our expression studies using the DNA demethylating agent showed that the *HOXA2*, *HOXA4*, and *HOXA7* genes were reactivated and

that the *HOXA2* gene was relatively resistant to derepression compared with the other genes. In fact, the promoter-associated CpG islands in these genes were highly methylated. Chromatin immunoprecipitation analyses revealed that both MBD1 and hPc2 were present in the promoter regions of *HOXA2*, whereas MBD1 was found in the *HOXA7* and *HOXA4* promoters. In agreement with these data, knockdown of MBD1 or hPc2 highly reactivated *HOXA2* and, to lesser extent, *HOXA7* and *HOXA4*. Interestingly, the expressed *HOXA10* gene promoter was unexpectedly CpG-methylated but not targeted by MBD1, suggesting the presence of an unknown localizing mechanism of MBD1. Thus, MBD1 and hPc2 have overlapping roles in the transcriptional silencing of the *HOXA* genes (Fig. 6*A*).

Coexistence of MBD1 and PcG Proteins in Heterochromatin Foci—In agreement with the interactions of MBD1 and PcG proteins, they appeared to be closely positioned at heterochromatin foci in the nuclei. The localizations of the deletion mutants of MBD1 and hPc2 revealed that the coexistence of these proteins at the heterochromatin foci is dependent on the *CXXC* domains of MBD1 and chromodomain of hPc2. Interestingly, hPc2ΔC, lacking the carboxyl-terminal region that recruits CtBP and the other components of PRC1, had a diffuse distribution in the nuclei, suggesting that the PcG foci depend on the formation of the PRC1 complex. Furthermore, the heterochromatin foci containing MBD1 and Ring1b were marked by trimethylation of H3K9 and H3K27. Importantly, the foci containing hPc2 and Ring1b were not affected by knockdown of MBD1. Similarly, the MBD1 foci did not change after knockdown of hPc2. In addition, hPc2 knockdown reduced the colocalization of MBD1 foci with the trimethyl H3K27 (27.3-10.0%), indicating that hPc2 is involved in the colocalization but not the formation of MBD1 foci These results suggest that the MBD1 foci and PcG foci are independently assembled and that both foci are likely to be overlaid through physical interactions between MBD1 and PcG proteins (Fig. 6*B*). Thus, MBD1 and PcG proteins have an overlapping role in colocalization of these heterochromatin foci. In addition, the number of PcG foci significantly increased under conditions of 5-aza-dC-induced hypomethylation, suggesting the possibility that the PcG foci compensate for the decrease in CpG methylation. This may be related to the overexpression of PcG proteins in certain cancers that frequently show genome-wide DNA hypomethylation (30, 46). Luciferase reporter assays revealed that, in contrast to the *CXXC* domains or chromodomain, full-length MBD1 or hPc2 alone showed strong repressive activity (data not shown), suggesting that these proteins each have repressive activities and cooperate by colocalizing at heterochromatin regions. Our results shed light on the close links between MBD1 and PcG proteins for transcriptional repression and heterochromatin foci formation.

Acknowledgments—We thank N. Saitoh and other members of our laboratory for helpful suggestions.

REFERENCES

1. Damelin, M., Ooi, S. K., and Bestor, T. H. (2006) *Nat. Struct. Mol. Biol.* **13,** 100–101
2. Taghavi, P., and van Lohuizen, M. (2006) *Nature* **439,** 794–795
3. Wade, P. A. (2001) *BioEssays* **23,** 1131–1137
4. Bird, A. (2002) *Genes Dev.* **16,** 6–21
5. Klose, R. J., and Bird, A. P. (2006) *Trends Biochem. Sci.* **31,** 89–97
6. Francis, N. J., and Kingston, R. E. (2001) *Nat. Rev. Mol. Cell Biol.* **2,** 409–421
7. Simon, J. A., and Tamkun, J. W. (2002) *Curr. Opin. Genet. Dev.* **12,** 210–218
8. Fuks, F. (2005) *Curr. Opin. Genet. Dev.* **15,** 490–495
9. Bestor, T. H. (2000) *Hum. Mol. Genet.* **9,** 2395–2402
10. Baylin, S. B. (2005) *Nat. Clin. Pract. Oncol.* **2,** Suppl. 1, 4–11
11. Fujita, N., Takebayashi, S., Okumura, K., Kudo, S., Chiba, T., Saya, H., and Nakao, M. (1999) *Mol. Cell. Biol.* **19,** 6415–6426
12. Ng, H. H., Jeppesen, P., and Bird, A. (2000) *Mol. Cell. Biol.* **20,** 1394–1406
13. Fujita, N., Shimotake, N., Ohki, I., Chiba, T., Saya, H., Shirakawa, M., and Nakao, M. (2000) *Mol. Cell. Biol.* **20,** 5107–5118
14. Hendrich, B., and Bird, A. (1998) *Mol. Cell. Biol.* **18,** 6538–6547
15. Fujita, N., Watanabe, S., Ichimura, T., Tsuruzoe, S., Shinkai, Y., Tachibana, M., Chiba, T., and Nakao, M. (2003) *J. Biol. Chem.* **278,** 24132–24138
16. Fujita, N., Watanabe, S., Ichimura, T., Ohkuma, Y., Chiba, T., Saya, H., and Nakao, M. (2003) *Mol. Cell. Biol.* **23,** 2834–2843
17. Ichimura, T., Watanabe, S., Sakamoto, Y., Aoto, T., Fujita, N., and Nakao, M. (2005) *J. Biol. Chem.* **280,** 13928–13935
18. Wang, H., An, W., Cao, R., Xia, L., Erdjument-Bromage, H., Chatton, B., Tempst, P., Roeder, R. G., and Zhang, Y. (2003) *Mol. Cell* **12,** 475–487
19. Jorgensen, H. F., Ben-Porath, I., and Bird, A. P. (2004) *Mol. Cell. Biol.* **24,** 3387–3395
20. Ringrose, L., and Paro, R. (2004) *Annu. Rev. Genet.* **38,** 413–443
21. Boyer, L. A., Plath, K., Zeitlinger, J., Brambrink, T., Medeiros, L. A., Lee, T. I., Levine, S. S., Wernig, M., Tajonar, A., Ray, M. K., Bell, G. W., Otte, A. P., Vidal, M., Gifford, D. K., Young, R. A., and Jaenisch, R. (2006) *Nature* **441,** 349–353
22. Lee, T. I., Jenner, R. G., Boyer, L. A., Guenther, M. G., Levine, S. S., Kumar, R. M., Chevalier, B., Johnstone, S. E., Cole, M. F., Isono, K., Koseki, H., Fuchikami, T., Abe, K., Murray, H. L., Zucker, J. P., Yuan, B., Bell, G. W., Herbolsheimer, E., Hannett, N. M., Sun, K., Odom, D. T., Otte, A. P., Volkert, T. L., Bartel, D. P., Melton, D. A., Gifford, D. K., Jaenisch, R., and Young, R. A. (2006) *Cell* **125,** 301–313
23. Orlando, V. (2003) *Cell* **112,** 599–606
24. Otte, A. P., and Kwaks, T. H. (2003) *Curr. Opin. Genet. Dev.* **13,** 448–454
25. Cao, R., and Zhang, Y. (2004) *Curr. Opin. Genet. Dev.* **14,** 155–164
26. Lund, A. H., and van Lohuizen, M. (2004) *Curr. Opin. Cell Biol.* **16,** 239–246
27. Levine, S. S., King, I. F., and Kingston, R. E. (2004) *Trends Biochem. Sci.* **29,** 478–485
28. Min, J., Zhang, Y., and Xu, R. M. (2003) *Genes Dev.* **17,** 1823–1828
29. Fischle, W., Wang, Y., Jacobs, S. A., Kim, Y., Allis, C. D., and Khorasanizadeh, S. (2003) *Genes Dev.* **17,** 1870–1881
30. Sparmann, A., and van Lohuizen, M. (2006) *Nat. Rev. Cancer* **6,** 846–856
31. Vire, E., Brenner, C., Deplus, R., Blanchon, L., Fraga, M., Didelot, C., Morey, L., Van Eynde, A., Bernard, D., Vanderwinden, J. M., Bollen, M., Esteller, M., Di Croce, L., de Launoit, Y., and Fuks, F. (2006) *Nature* **439,** 871–874
32. Mager, J., Montgomery, N. D., de Villena, F. P., and Magnuson, T. (2003) *Nat. Genet.* **33,** 502–507
33. Hernandez-Munoz, I., Taghavi, P., Kuijl, C., Neefjes, J., and van Lohuizen, M. (2005) *Mol. Cell. Biol.* **25,** 11047–11058
34. Nakamura, T., Mori, T., Tada, S., Krajewski, W., Rozovskaia, T., Wassell, R., Dubois, G., Mazo, A., Croce, C. M., and Canaani, E. (2002) *Mol. Cell* **10,** 1119–1128
35. Milne, T. A., Briggs, S. D., Brock, H. W., Martin, M. E., Gibbs, D., Allis, C. D., and Hess, J. L. (2002) *Mol. Cell* **10,** 1107–1117
36. Xia, Z. B., Anderson, M., Diaz, M. O., and Zeleznik-Le, N. J. (2003) *Proc. Natl. Acad. Sci. U. S. A.* **100,** 8342–8347
37. Watanabe, S., Ichimura, T., Fujita, N., Tsuruzoe, S., Ohki, I., Shirakawa, M., Kawasuji, M., and Nakao, M. (2003) *Proc. Natl. Acad. Sci. U. S. A.* **100,** 12859–12864
38. Jones, P. A., and Baylin, S. B. (2002) *Nat. Rev. Genet.* **3,** 415–428

39. Herman, J. G., and Baylin, S. B. (2003) *N. Engl. J. Med.* **349,** 2042–2054
40. Shiraishi, M., Sekiguchi, A., Oates, A. J., Terry, M. J., and Miyamoto, Y. (2002) *Oncogene* **21,** 3659–3662
41. Terranova, R., Agherbi, H., Boned, A., Meresse, S., and Djabali, M. (2006) *Proc. Natl. Acad. Sci. U. S. A.* **103,** 6629–6634
42. Schoorlemmer, J., Marcos-Gutierrez, C., Were, F., Martinez, R., Garcia, E., Satijn, D. P., Otte, A. P., and Vidal, M. (1997) *EMBO J.* **16,** 5930–5942
43. Sewalt, R. G., Gunster, M. J., van der Vlag, J., Satijn, D. P., and Otte, A. P. (1999) *Mol. Cell. Biol.* **19,** 777–787
44. Peters, A. H., Kubicek, S., Mechtler, K., O'Sullivan, R. J., Derijck, A. A., Perez-Burgos, L., Kohlmaier, A., Opravil, S., Tachibana, M., Shinkai, Y., Martens, J. H., and Jenuwein, T. (2003) *Mol. Cell* **12,** 1577–1589
45. Sarraf, S. A., and Stancheva, I. (2004) *Mol. Cell* **15,** 595–605
46. Ehrlich, M. (2002) *Oncogene* **21,** 5400–5413

Cell Death and Differentiation (2007) 14, 1475–1485

www.nature.com/cdd

Aberrant quality control in the endoplasmic reticulum impairs the biosynthesis of pulmonary surfactant in mice expressing mutant BiP

N Mimura[1,2], H Hamada[3], M Kashio[1], H Jin[1], Y Toyama[4], K Kimura[2], M Iida[5], S Goto[2], H Saisho[2], K Toshimori[4], H Koseki[5] and T Aoe*[,1]

Accumulation of misfolded proteins in the endoplasmic reticulum (ER) induces the unfolded protein response (UPR), which alleviates protein overload in the secretory pathway. Although the UPR is activated under diverse pathological conditions, its physiological role during development and in adulthood has not been fully elucidated. Binding immunoglobulin protein (BiP) is an ER chaperone, which is central to ER function. We produced knock-in mice expressing a mutant BiP lacking the retrieval sequence to cause a defect in ER function without completely eliminating BiP. In embryonic fibroblasts, the UPR compensated for mutation of BiP. However, neonates expressing mutant BiP suffered respiratory failure due to impaired secretion of pulmonary surfactant by alveolar type II epithelial cells. Expression of surfactant protein (SP)-C was reduced and the lamellar body was malformed, indicating that BiP plays a critical role in the biosynthesis of pulmonary surfactant. Because pulmonary surfactant requires extensive post-translational processing in the secretory pathway, these findings suggest that in secretory cells, such as alveolar type II cells, the UPR is essential for managing the normal physiological ER protein overload that occurs during development. Moreover, failure of this adaptive mechanism may increase pulmonary susceptibility to environmental insults, such as hypoxia and ischemia, ultimately leading to neonatal respiratory failure.
Cell Death and Differentiation (2007) **14,** 1475–1485; doi:10.1038/sj.cdd.4402151; published online 20 April 2007

Secretory proteins are subjected to quality control in the endoplasmic reticulum (ER) through interaction with molecular chaperones such as binding immunoglobulin protein (BiP), which functions as intermediaries for protein folding or degradation.[1] Extracellular insults, such as ischemia, hypoxia, and genetic mutations, result in aberrant protein folding and accumulation of misfolded proteins in the ER. ER stress initiates the unfolded protein response (UPR), which enhances the capacity for ER quality control by reducing general protein synthesis, producing ER chaperones, and promoting ER-associated protein degradation (ERAD).[2,3] Failure of this adaptive mechanism can cause cellular dysfunction and cell death, resulting in diverse human disorders[4,5] such as neurodegenerative disease, cardiomyopathy,[6] and diabetes.[7]

Respiratory distress syndrome in newborns is often associated with premature birth or low birth weight accompanied by reduced pulmonary surfactant production.[8] Pulmonary surfactant is secreted by highly differentiated alveolar type II epithelial cells, and is composed of phospholipids and surfactant proteins (SP) A, B, C, and D. Surfactant reduces alveolar surface tension and keeps the alveolar space open, which is essential for lung function after the transition at birth from the embryonic fluid environment to air. SP-B and SP-C are small, highly hydrophobic proteins processed from proSP-B and proSP-C, respectively, during transport through the ER and the Golgi to the multivesicular body. Mature SP-B and SP-C are further transported to the lamellar body where they bind phospholipids before secretion into the alveolar space via regulated exocytosis. ProSP-B associated with BiP is found in the ER.[9] Furthermore, mutations in SP-C cause the accumulation of misfolded SP-C in the ER, thereby activating the UPR,[10,11] resulting in interstitial lung disease in children and adults. This suggests that ER stress is involved in lung disease,[12] but whether ER dysfunction causes lung disease remains an open question.

BiP, one of the most abundant ER chaperones, plays a central role in ER function, assisting in protein translocation, folding, degradation, and regulation of the UPR.[13] ER chaperones are localized to the ER by two mechanisms — retention and retrieval.[14] BiP is retained in the ER through interaction with other ER proteins and the ER matrix. When misfolded proteins accumulate in the ER, BiP dissociates from some ER membrane proteins, such as inositol-requiring kinase-1 (IRE1), PKR-like ER-associated kinase (PERK), and activating transcription factor 6 (ATF6). BiP dissociation activates

[1]Department of Anesthesiology, Chiba University Graduate School of Medicine, 1-8-1 Inohana, Chuo-ku, Chiba City, Chiba, Japan; [2]Department of Medicine and Clinical Oncology, Chiba University Graduate School of Medicine, 1-8-1 Inohana, Chuo-ku, Chiba City, Chiba, Japan; [3]Department of Pediatrics, Chiba University Graduate School of Medicine, 1-8-1 Inohana, Chuo-ku, Chiba City, Chiba, Japan; [4]Department of Anatomy and Developmental Biology, Chiba University Graduate School of Medicine, 1-8-1 Inohana, Chuo-ku, Chiba City, Chiba, Japan; [5]Laboratory for Developmental Genetics, RIKEN Research Center for Allergy and Immunology, 1-7-22 Suehiro, Tsurumi, Yokohama, Japan
*Corresponding author: T Aoe, Department of Anesthesiology, Chiba University Graduate School of Medicine, 1-8-1 Inohana, Chuo-ku, Chiba City, Chiba 260-8670, Japan. Tel: +81 43 226 2573; Fax: +81-43-226-2156; E-mail: taoe@faculty.chiba-u.jp
Keywords: chaperone; endoplasmic reticulum; pulmonary surfactant; respiratory failure; UPR
Abbreviations: BiP, binding immunoglobulin protein; ER, endoplasmic reticulum; ERAD, ER-associated protein degradation; MEF, mouse embryonic fibroblast; PAS, periodic acid Schiff; SP, surfactant protein; UPR, unfolded protein response
Received 09.8.06; revised 15.2.07; accepted 16.3.07; Edited by M Piacentini; published online 20.4.07

these kinases and transcription factors and initiates the UPR,[15] which leads to increased expression of X-box-binding protein-1 (XBP-1) and ATF4.[3] When BiP is secreted from the ER along with misfolded proteins,[16,17] the C-terminal Lys-Asp-Glu-Leu (KDEL) sequence of BiP is recognized by the KDEL receptor, thereby facilitating the retrieval of BiP from post-ER compartments to the ER.[18,19] Yeast BiP (Kar2) is essential for survival; when the retrieval sequence (in yeast: His-Asp-Glu-Leu, HDEL) is deleted, a fraction of Kar2 is secreted from the ER. However, the UPR is activated and this maintains a minimal level of Kar2 in the ER.[20]

Complete depletion of BiP could be lethal for early embryonic cells.[21] We therefore produced knock-in mice expressing a mutant BiP in which the retrieval sequence was deleted by homologous recombination. These mice were used to elucidate processes sensitive to ER stress during development and in adulthood. The mutant-BiP mice died several hours after birth. Analysis of neonatal mutants revealed that dedicated secretory systems essential for pulmonary development might include an adaptive mechanism whereby BiP function accommodates increased levels of secretory proteins.

Results

Constitutively active UPR compensates for loss of ER BiP in cultured mammalian cells. We used homologous recombination to produce knock-in mice expressing a mutant BiP lacking the C-terminal KDEL sequence (Figure 1). This mutant BiP contained a C-terminal HA tag. Mouse embryonic fibroblasts (MEFs) derived from homozygous BiP mutant embryos expressed mutant BiP instead of wild-type BiP but grew as well as wild-type MEFs. Mutant BiP localized to the ER, and its expression was enhanced by tunicamycin, which disrupts protein glycosylation in the ER, thereby inducing the UPR. These results are consistent with those for wild-type BiP and other ER chaperones containing a KDEL sequence (Figure 2a). However, in metabolic labeling experiments, a significant fraction of mutant BiP was found in the medium, reflecting deletion of the KDEL sequence and impaired retrieval of mutant BiP (Figure 2b). We estimate that under resting culture conditions, one-third of the newly synthesized mutant BiP was secreted. The remainder was retained in the ER. A fraction of wild-type BiP was also secreted into the medium during ER stress (tunicamycin treatment), indicating that retrieval by the KDEL receptor is saturable.

Tunicamycin sensitivity and expression of mutant BiP was also confirmed by Western blotting (Figure 3a and b). Both mutant BiP and wild-type BiP were recognized by an antibody against the N-terminus of BiP. However, anti-KDEL only recognized wild-type BiP and GRP94, an ER chaperone with the KDEL sequence. Basal expression of XBP1, ATF4, phospho-PERK, and another ER chaperone, calreticulin, was enhanced in homozygous mutant BiP MEFs. Basal expression of mutant BiP mRNA was also enhanced in mutant MEFs (Figure 3c), indicating that the UPR was constitutively active. Thus, as seen previously in yeast,[20] constitutive UPR activation maintains a minimal level of BiP (mutant or wild type) in the ER of mammalian cells, thus compensating for deletion of the KDEL sequence.

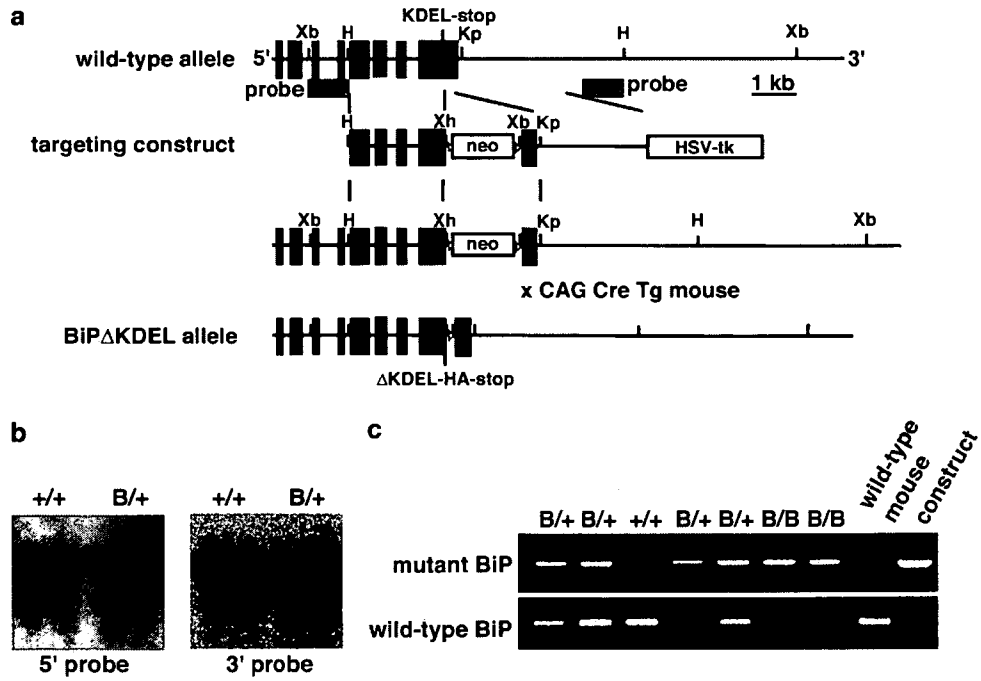

Figure 1 Generation of knock-in mice expressing a mutant BiP lacking the KDEL retrieval sequence. (**a**) Top, the wild-type allele containing the BiP gene. Exons are indicated as solid bars. Middle, the targeting vector for homologous recombination. Bottom, the recombinant allele. The external probes for Southern blot analysis are indicated by gray quadrangle. Xb, *Xba*I; H, *Hin*dIII; B, *Bam*HI; Kp, *Kpn*I; Xh, *Xho*I. (**b**) Southern blots of ES cell genomic DNA digested with *Xba*I. The 5′ external probe detected a 11.2-kb fragment in the wild-type allele and a 4.7-kb fragment in the mutant allele. The 3′ external probe detected a 11.2-kb fragment in the wild-type allele and a 8.0-kb fragment in the mutant allele. '+' represents the wild-type allele, and 'B' represents the mutant allele. (**c**) Genotyping of mice by PCR

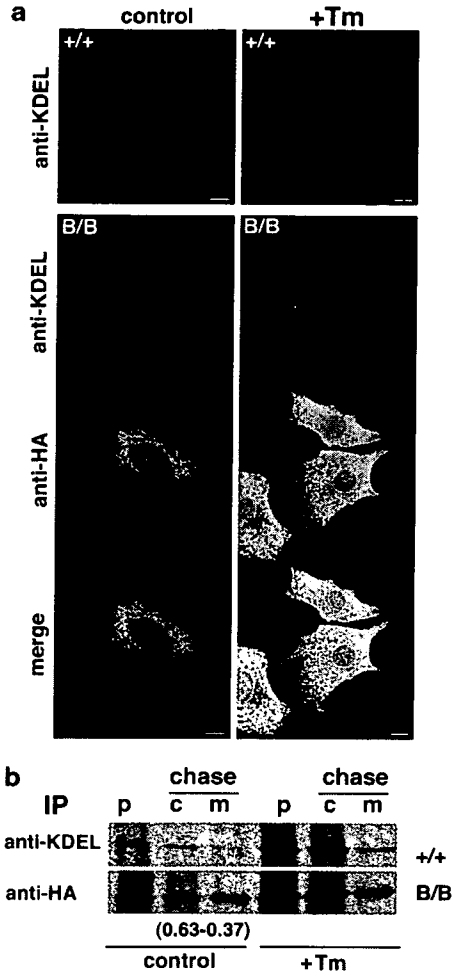

Figure 2 Deletion of the KDEL sequence impairs retrieval of mutant BiP. (**a**) MEFs from homozygous mutant (B/B) and wild-type (+/+) embryos treated with or without tunicamycin (Tm, 2.5 μg ml^{-1}) for 12 h were double-stained with monoclonal anti-KDEL and polyclonal anti-HA and observed by confocal laser microscopy. The anti-KDEL recognizes BiP as well as other KDEL-containing proteins, such as GRP94. Scale bars represent 10 μm. (**b**) Tm-treated (2.5 μg ml^{-1} for 12 h) or untreated MEFs were subjected to pulse-chase (p and c) labeling with[35S]methionine. Proteins in cell lysates (p and c) and in the culture medium (m) were immunoprecipitated with anti-KDEL or anti-HA. The proportion of secreted mutant BiP (m; 0.37) was evaluated by densitometry

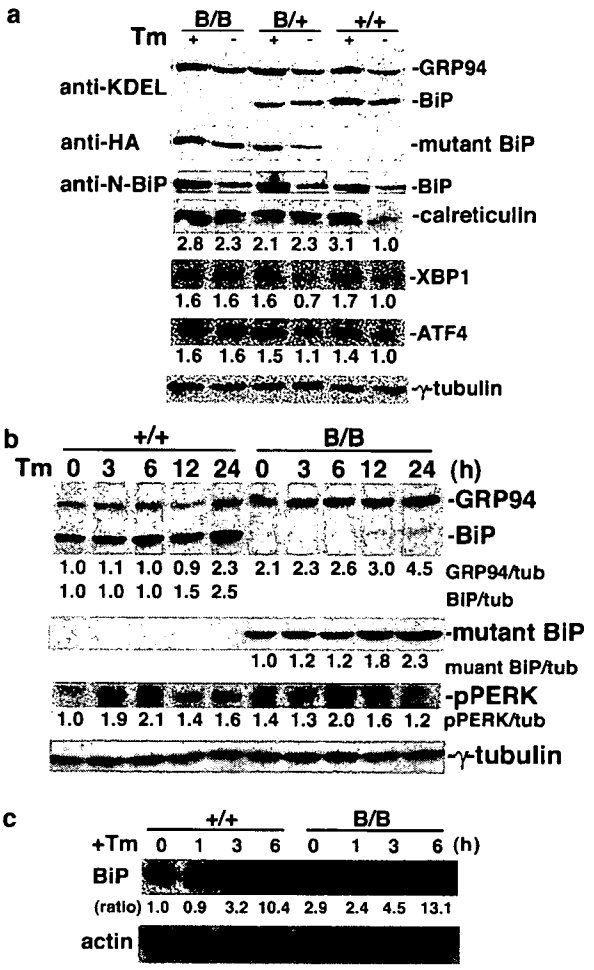

Figure 3 Loss of wild-type BiP is compensated by constitutive activation of the UPR in mammalian cells. (**a**) Tunicamycin (Tm)-treated (2.5 μg ml^{-1} for 12 h) or untreated MEFs from homozygous (B/B), heterozygous (B/+) and wild-type (+/+) embryos were collected. Expression of BiP, GRP94, mutant BiP, calreticulin, XBP1, ATF4, and γ-tubulin was determined by Western blotting. (**b**) Tm-treated (2.5 μg ml^{-1} for 0, 3, 6, 12, and 24 h) MEFs from homozygous (B/B) and wild-type (+/+) embryos were collected. Expression of BiP, GRP94, mutant BiP, phospho-PERK, and γ-tubulin was determined by Western blotting. The expression of each protein was normalized to that of γ-tubulin. (**c**) Northern blot of BiP mRNA expression in MEFs from homozygous (B/B) and wild-type (+/+) embryos treated with Tm (2.5 μg ml^{-1}) at 37°C for 0–6 h. The expression of BiP mRNA was normalized to that of β-actin mRNA

Mutant-BiP embryos die shortly after birth. BiP was ubiquitously expressed in both mutant and wild-type embryos (Figure 4a and b). In all tissues examined, GRP94 expression was greater in homozygous BiP mutant embryos than in wild-type embryos (Figure 4b), suggesting that homozygous BiP mutant mice may suffer from global ER stress. Homozygous mutant-BiP embryos weighed less than wild types and heterozygotes at embryonic day (E) 18.5 (Figure 4c). Homozygous BiP mutant mice, shown in Figure 4d, were born at the expected Mendelian ratio of 1:2:1 (84:182:90, wild type:heterozygous:homozygous). Neonatal BiP mutants moved well and responded to painful stimuli, but they appeared pale and cyanotic. They also cried less and displayed shallow breathing. The neonatal homozygous mutants generally died within several hours of birth; thus, we suspected that the observed lethality might reflect respiratory problems.

When delivered by Caesarian section at E18.5 and killed before breathing, gross morphology of the lungs (Figure 4e) and airways from BiP mutant mice was indistinguishable from wild type (Figure 5a). Wild-type and homozygous BiP mutant embryonic alveoli had an equivalent distribution of alveolar type II cells expressing the SP-C (Figure 5b). However, histological examination of lungs isolated from neonatal BiP mutants several hours after birth revealed atelectasis with poor inflation of peripheral airways. Hemorrhage and cell debris were also observed in the mutant alveolar space. Alveolar epithelia in BiP mutant mice were enlarged, whereas, as expected, those in wild-type neonates were distended

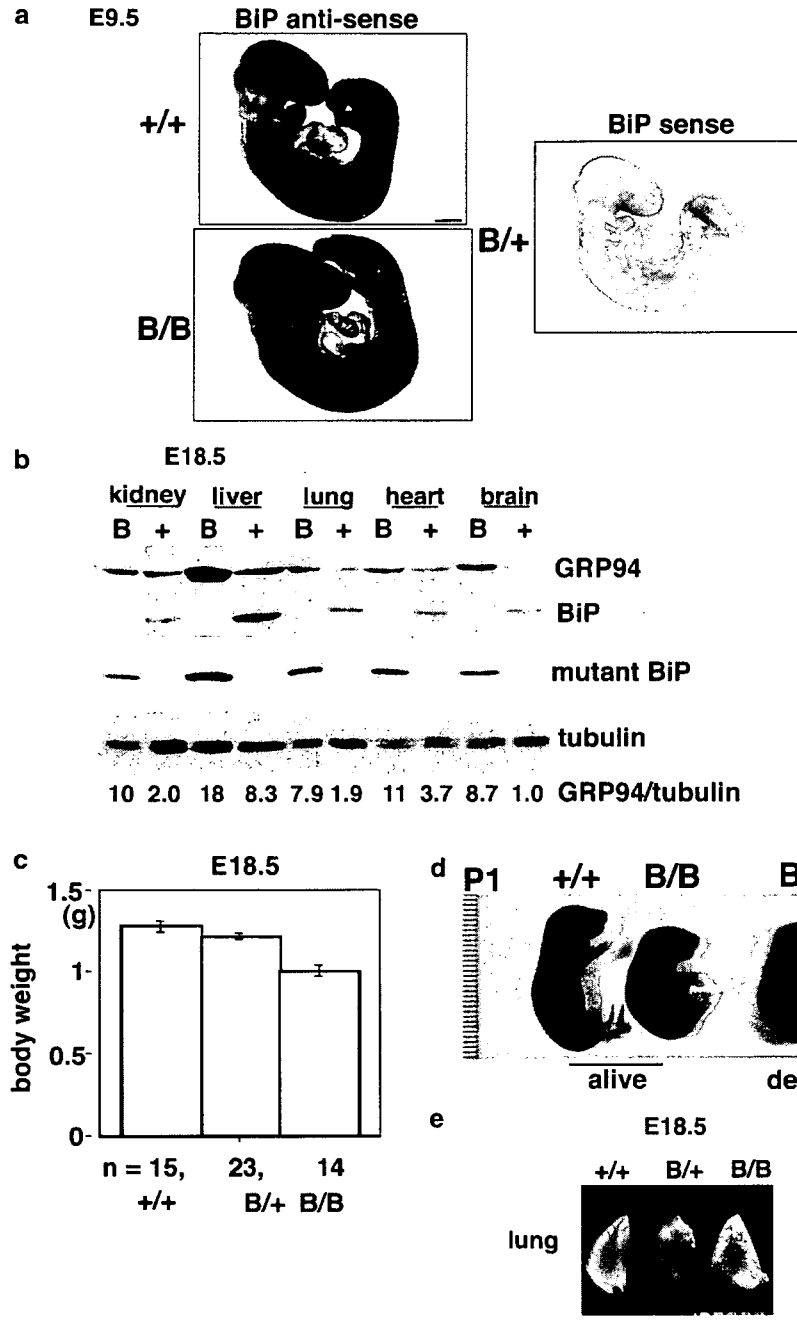

Figure 4 Mutant-BiP embryos die shortly after birth. (**a**) BiP expression was ubiquitous in both mutant and wild-type embryos. Whole-mount *in situ* hybridization revealed ubiquitous expression of BiP and mutant BiP in E9.5 embryos. Scale bar represents 200 μm. (**b**) Western blots of BiP or mutant-BiP in tissues from wild type (+) and homozygous mutant (**b**) E18.5 embryos, respectively. Expression of GRP94 was normalized to that of γ-tubulin. In all tissues examined, GRP94 was greater in mutants than in wild type. (**c**) Body weights (mean $\pm$ S.D.) of homozygous (B/B, $n=14$), heterozygous (B/+, $n=23$) and wild-type (+/+, $n=15$) E18.5 embryos. Homozygous mutant embryos weighed significantly less than wild types or heterozygotes ($P<0.0001$). (**d**) Gross appearance of wild type (+/+) and homozygous (B/B) P1 neonates. (**e**) Lungs from E18.5 mice delivered by Cesarian section

(Figure 5c). These observations indicate that homozygous neonatal BiP mutants developed atelectasis and respiratory failure after birth.

Altered biosynthesis of SPs in mutant alveolar type II cells. To examine whether a deficiency of pulmonary surfactant contributes to respiratory failure in homozygous BiP mutant mice, perfluorocarbon, a substitute for pulmonary surfactant, was administered into the oropharynx. Perfluorocarbon with oxygen treatment improved the activity of neonatal BiP mutants, turned their skin color from pale to pink, and improved lung inflation (Figure 5d). Expression of SPs in neonatal lung was examined by Western blotting (Figure 6a). Expression of SP-A and, more prominently,

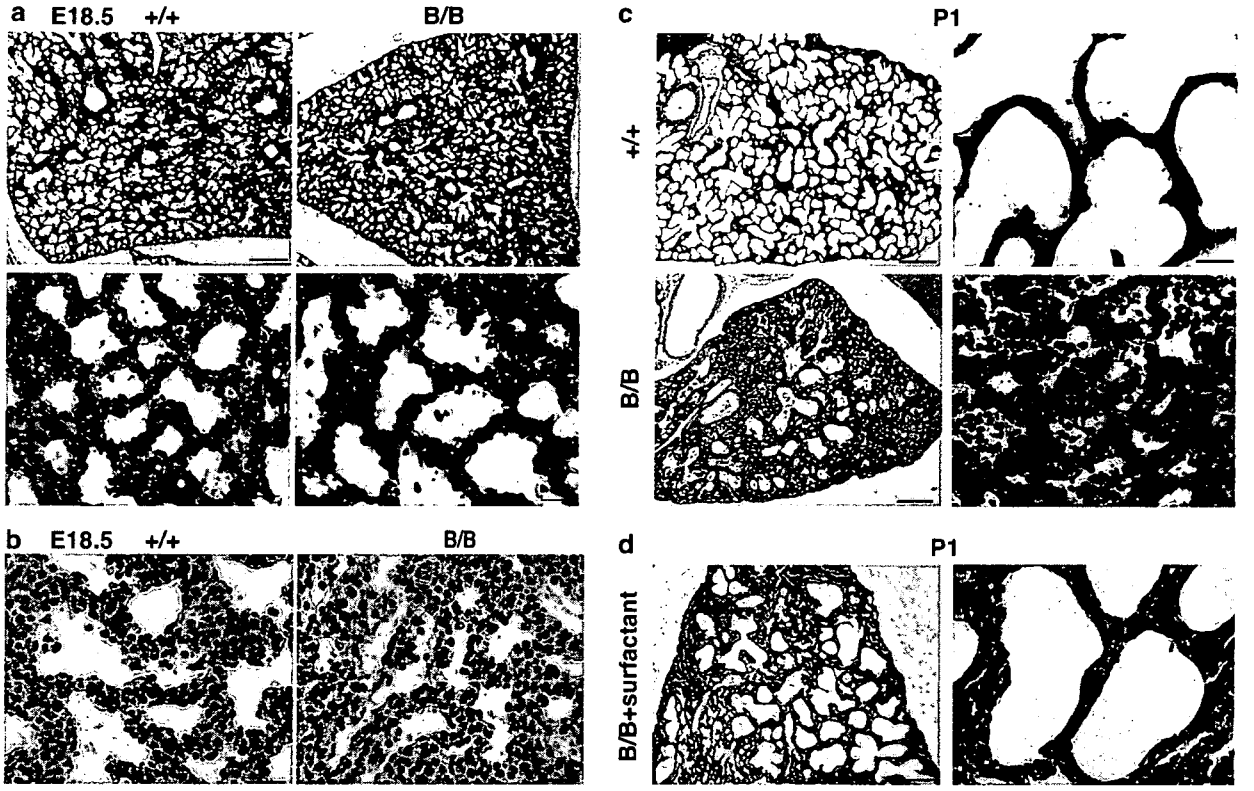

Figure 5 The gross morphology of lungs and airways from BiP mutant embryos is indistinguishable from wild type. (**a**, **b**) Lungs from E18.5 mice delivered by Cesarian section. (**a**) Sections stained with hematoxylin and eosin. +/+: wild-type, B/B: homozygous mutant. (**b**) Alveolar type II epithelial cells were stained with anti-SP-C (brown). Nuclei were stained with hematoxylin (violet). (**c**) Lung sections from P1 neonates. Atelectasis and cell debris were evident in the peripheral airways of neonatal mutants. +/+: Wild-type, B/B: homozygous mutant. (**d**) Lungs from a P1 neonatal BiP mutant (B/B) administered 50 μl of perfluorocarbon via the oropharynx and treated with 40% oxygen for 6 h. Sections were stained with hematoxylin and eosin. Scale bars represent 200 and 20 μm in the low- and high-magnification images, respectively

proSP-C, was reduced in mutant lungs compared with wild type, but there was no significant difference in proSP-B and SP-D expression. RT-PCR analysis revealed that the marked reduction of proSP-C in neonatal mutant lung was not due to reduced transcription (Figure 6b). Importantly, after birth, the expression of proSP-C was enhanced only in wild-type neonates (Figure 6c), suggesting that proSP-C might be degraded post-translationally in neonatal type II cells from BiP mutants. Furthermore, expression of CHOP, a transcription factor related to cell death during ER stress,[22] increased in homozygous mutant lungs after birth, suggesting that mutant lung tissue might be suffering from ER stress. Heterozygous BiP mutants were viable and grew to adulthood. Furthermore, heterozygous expression of wild-type BiP sustained SP-C expression and suppressed CHOP expression in lung (Figure 6d and e), suggesting that the wild-type BiP is essential for SP-C biosynthesis.

The subcellular localization of SP-A and SP-C was evaluated by confocal laser microscopy. In wild-type neonatal alveolar type II cells, SP-A and SP-C (proSP-C) colocalized with BiP, and other KDEL sequence–containing ER chaperones, in the ER. SP-A accumulated in the alveolar lining area of BiP mutant mice and costained with mutant BiP (Figure 7a). By contrast, SP-C remained in the ER, and its expression was markedly reduced in type II cells of neonatal BiP mutants (Figure 7b). Mature SP-B and SP-C are transported to the lamellar body where they bind phospholipids and are then secreted into the alveolar space via regulated exocytosis, whereas SP-A and SP-D are secreted independently of the lamellar body.[12] Together, these data suggest that mutant BiP impairs the secretion of pulmonary surfactant, especially secretion through the lamellar body.

Embryonic type II cells store glycogen in the cytoplasm, and this glycogen is consumed as the synthesis of pulmonary surfactant expands after birth. Type II cells in neonatal BiP mutants contained vacuole structures. Periodic acid Schiff (PAS) staining revealed cytoplasmic polysaccharides in these cells, even after birth (Figure 8a). Ultrastructural analysis of type II cells from neonates confirmed that cytoplasmic glycogen was indeed still present in mutant, but not in wild type, cells (Figure 8b and c). More importantly, the structure of the lamellar body was abnormal in embryonic and neonatal mutant type II cells. The lamellar body in wild-type neonates had wavy, dense laminations with clefting, whereas in BiP mutant neonates the lamellar body had loosely formed lamellar structures or was almost empty. These results indicate that the biosynthesis and secretion of pulmonary surfactant was impaired in BiP mutant type II cells.

SP-C is a small, highly hydrophobic protein processed from proSP-C during its transport through the ER and the Golgi to the multivesicular body. Mature SP-C is transported further to the lamellar body where it binds phospholipids before